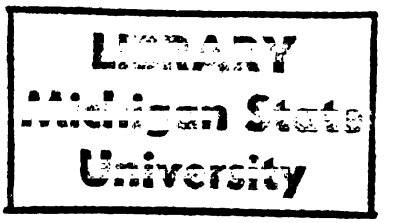

This is to certify that the

thesis entitled

SYNTHESIS OF YTTERBIUM DIHALIDES
AND AN X-RAY DIFFRACTION STUDY OF
YTTERBIUM MIXED DIHALIDE SYSTEMS

presented by

Christine Voos-Esquivel

has been accepted towards fulfillment
of the requirements for

M.S. degree in Chemistry

Harry A Eick
Major professor

Date 2-14-'82

SYNTHESIS OF YTTERBIUM DIHALIDES AND AN X-RAY DIFFRACTION STUDY OF YTTERBIUM MIXED DIHALIDE SYSTEMS

By

Christine A. Voos-Esquivel

A THESIS

Submitted to
Michigan State University
in partial fulfillment of the requirements
for the degree of

MASTER OF SCIENCE

Department of Chemistry

1986

ABSTRACT

SYNTHESIS OF YTTERBIUM DIHALIDES AND AN X-RAY DIFFRACTION STUDY OF YTTERBIUM MIXED DIHALIDE SYSTEMS

By

Christine Voos-Esquivel

Many diverse synthetic routes have been developed for the preparation of ytterbium dihalides. Most of these routes either involve multistep reactions or are otherwise complicated.

In this work a high temperature synthetic procedure was developed for the preparation of $YbCl_2$ and $YbBr_2$, and a low temperature procedure for the preparation of YbI_2.

The pure ytterbium dihalides were combined by high temperature fusion techniques to produce mixed halides and the mixed halide systems; YbI_2-$YbCl_2$, YbI_2-$YbBr_2$ and $YbCl_2$-$YbBr_2$ were characterized by x-ray diffraction. The $YbCl_2$-$YbBr_2$ system exhibited the SrI_2-type structure throughout the entire composition region. In the other two mixed halide systems, new phases were identified but not characterized. Phase diagrams are presented and are compared to those observed in other mixed halide systems.

ACKNOWLEDGMENTS

I acknowledge the professors at Virginia Tech., especially Dr. Taylor, Dr. Ogliaruso, Dr. Bell, Dr. Kingston, Dr. Wightman and Dr. McNair. They taught me the fundamentals of chemistry. A special acknowledgment goes to Dr. Mason. His encouragement helped me to continue my pursuit of a chemistry degree.

Turning to Michigan State, Dr. Harrison's role as a teacher gave me a different perspective of chemistry, and his role as advisor helped me to surmount some seemingly impossible obstacles.

To Dr. Eick, he assumed many roles including teacher, advisor and research director. He has been a major factor in transforming my dream of becoming a chemist into a tangible degree.

And lastly, to my husband, Benjamin, whose emotional and psychological support has always been constant throughout my five year struggle.

I thank you. All of you have been a major influence in my growth as a chemist.

I would like to acknowledge the support provided by the National Science Foundation, Division of Materials Research (DMR 84-00739).

TABLE OF CONTENTS

LIST OF TABLES

LIST OF FIGURES

INTRODUCTION

Practical Uses

Alkyl ytterbium dihalides are used as grignard-type[46] reagents in organometallic chemistry. The grignard reagent has the general formula of RMgX (R = alkyl, X = halide).

A typical reaction of RMgX is with aldehydes and ketones to yield alcohols. The R group functions as a nucleophile which readily transfers its electrons to the electropositive carbon of the carbonyl group of a specific ketone or aldehyde. The electrophilic portion, MgX, attacks the oxygen of the carbonyl group. Finally, the addition of water removes the MgX and an alcohol is formed.

Before 1977, lanthanide dihalides were generally synthesized by reduction of the trihalide with hydrogen or a metal at high temperatures. In 1977, a room temperature preparatory procedure was reported[38] in which ytterbium metal reacts with THF solutions of 1,2-diiodoethane.

The reactivities of these powerful reducing agents, YbX_2, have been applied[21] to conjugated double bond compounds such as cinnamic acid which have been reduced to 3-phenylpropionic acid. Octanal can be converted to 1-octanol. By an exchange reaction, new divalent compounds, such as $Yb(OEt)_2$ and $Yb(OAc)_2$[25] were synthesized by use of YbI_2 as an intermediate and RONa (R = Et or Ac) as a reactant.

Recently, ytterbium metal has been explored for use as a catalyst.[24] Butadiene has been reduced to butenes at 20-64°C by a Yb-Ar-THF matrix and hydrogen.

General Background

Ytterbium metal is a powerful reducing agent, ($Yb^{+3} + 3e^- \rightarrow Yb$, $E^\circ = -2.27$ V)($Yb^{+3} + e^- \rightarrow Yb^{+2}$, $E^\circ = -1.21$ V). In all MSU synthetic preparations, oxidation of ytterbium by the metal halogen compound was pursued (for example, $Yb + ZnCl_2 \rightarrow YbCl_2 + Zn$).

Ytterbium can be considered a transition metal by the following arguments. Another metal, lanthanum is placed in the periodic chart in group IIIB position, but Jenson[28](1982) and other chemists put lutetium in this place.

In the case of lutetium, the highest common oxidation state is +3 with a $[Xe]4f^{14}$ electron configuration. Likewise, one common oxidation state for ytterbium is +2 with a $[Xe]4f^{14}$ electron configuration. If Lu can be considered a transition element due to its $[Xe]6s^24f^{14}5d^1$ electron configuration, and is placed in group IIIB with Sc $[Ar](3d^14s^2)$ and Y $[Ar](4d^15s^2)$, then ytterbium 2+ can likewise be considered a transition metal based on the comparison of the electron configuration of Yb(+2) to Lu(+3). La would be placed at the beginning of the lanthanide series instead of Ce.

Atomic radii, ionization potential, and electronegativity trends of the Sc-Y-Lu group versus those of other transition metal groups support Lu being in the group IIIB position. The elements Sc, Y and Lu have the following common properties: oxidation state, structure of the metal at room temperature, structure of the oxide and structure of the chloride. The elements Sc, Y and La don't have these common properties.

Goals

By continuing to pursue an understanding of new phase formation of mixtures of two solids, the area of solid state chemistry with practical applications in material science will be explored through the following goals:

1. Development of a one-step, fast high temperature preparatory procedure for $YbCl_2$. All reported preparations involve one or more of the following:

   1) two step reactions

   2) extended time period (one week)

   3) special conditions--low temperature or solvents

2. Development of a one-step high temperature preparatory procedure for $YbBr_2$. All reported preparations involve low temperature techniques, solvents at room temperature or two-step reactions.

3. Development of a one-step low temperature preparatory procedure for YbI_2. All reported preparations involve one or more of the following:

   1) $Yb(s) + I_2(g)$ which is potentially hazardous

   2) low temperature

   3) room temperature with solvents

4. Characterization by X.R.D. (x-ray diffraction) of the high temperature mixed halide systems: YbI_2-$YbCl_2$; YbI_2-$YbBr_2$ and $YbCl_2$-$YbBr_2$. Identification of and reasons for new phase formation will be examined.

HISTORICAL

General Synthetic Methods

This historical section presents an extensive chronological review of reported synthetic techniques for both ytterbium dihalides and trihalides. This section ends with a summary of ytterbium dihalide and trihalide preparatory procedures.

Unusual oxidation states of selected actinide and lanthanide elements including ytterbium are discussed in a 1960 review article.[21] The first reported preparation of $YbCl_2$ was that of Klemm and Schuth (1929)[27] by hydrogen reduction of $YbCl_3$ at 600–620°C.

Taylor (1962)[1] discussed the preparation of anhydrous lanthanide halides from lanthanide oxides or hydrates. He presented a comprehensive summary of all the published work up to 1961.

At that time, pure lanthanide metals were not available, so direct metal-halogen synthetic routes were impossible. Lanthanide trichlorides were synthesized by dehydration of hydrated trichlorides in a stream of HCl at 350°C or NH_4Cl at 300°C or by conversion of oxides by use of S_2Cl_2 and Cl_2 at 700–800°C. Also, lanthanide oxide has been added to CCl_4 at 400–500°C. Reported lanthanide tribromide preparations involved treatment of hydrated bromide salts with HBr at 600°C and NH_4Br at 350°C. Lanthanide triiodides were prepared by conversion of the oxide by NH_4I at 350°C.

Lanthanide trihalides, LnX_3, were produced when lanthanide oxide was combined with NH_4X and HX, where X = Cl, Br or I as indicated in a later literature report.[2] These reactants were combined in a beaker, dissolved to produce a clear solution, and subsequently evaporated to dryness on a hot plate. The resulting solid was transferred to a Pyrex glass tube which was evacuated. The tube was placed in an oven and heated to 200°C so the starting materials can react. During this heating, water was also removed. The temperature was then increased to 430°C to sublime the ammonium halide. After cooling the tube and filling it with nitrogen, the lanthanide halide was removed to a dry box.

A similar procedure was used successfully for preparation of all lanthanide halides except SmI_3 and EuI_3.

To determine the vapor pressure of $YbCl_2$,[3] ytterbium dichloride was synthesized from $YbCl_3$, mixed with a two fold excess of Zn in a quartz ampoule which was coated internally with molybdenum, evacuated and filled with argon. These reactants were heated at 900-950°C for 30 min. The $YbCl_3$ was made by the addition of chlorine gas to Yb_2O_3 at 600-700°C.

Lanthanide triiodides were prepared by the reaction of elemental lanthanides with HgI_2 at 500°C for 2 hours.[4] YbI_3 could not be prepared by this procedure, but was synthesized by confining elemental I_2 and Yb in a thick walled quartz tube. The quartz tube was cooled in an ice bath, evacuated and sealed. This sealed ampoule was placed in a capped steel pipe to prevent damage in case of an explosion, and the assembly was heated in a muffle furnace at 500°C.

$YbCl_3$ was synthesized[5] for a dissociation pressure measurement by the reaction of ytterbium oxide in a stream of chlorine gas saturated with CCl_4 vapor. This reaction took place in a tubular furnace at 700-720°C for 10-15 hours.

Howell and Pytlewski (1969) wrote two papers, one on the synthesis of divalent europium and ytterbium halides in liquid ammonia[8] and the other on the decomposition products of both metals in liquid ammonia.[9] Yb and Eu halides were made by the following reaction:

$$M + 2NH_4X \xrightarrow{liq.NH_3} MX_2 + 2NH_3 + H_2$$

$$M = Eu, Yb; X = Cl, Br, I$$

Each metal-halogen compound was analyzed for metal, halogen, nitrogen and hydrogen content. In the $YbBr_2$ and $YbCl_2$ analyses, 0.05%

and 0.2%, respectively, were not accounted for. Oxygen could be a likely contaminant as shown from the MSU experimental work. For the YbI_2 synthesis, the analysis showed a 0.44% excess which could be hydrate by-products.

A further extension of the Taylor procedure[2] for preparation of $YbCl_2$ was tried.[10] In the DeKock and Radtke procedure,[10] the appropriate metal oxide is added to HCl, NH_4Cl and $ZnCl_2$. Then, this mixture is evaporated to dryness. Elemental zinc is added to the resulting solid which is placed in a quartz tube and heated at 200°C under vacuum to remove H_2O and excess NH_4Cl. A metal and chlorine analysis showed 0.41% not accounted for. Again, oxygen could have been a by-product.

Anhydrous ytterbium trichloride and dichloride were made by the following procedures:[11]

1. Hydrated ytterbium trichloride was placed in a vitreosil boat which was situated in a silica combustion tube through which anhydrous hydrogen chloride was passed. The temperature was increased slowly to 150°C. The flow of the HCl gas was stopped and the pressure inside the tube was reduced to remove the water. The result was anhydrous $YbCl_3$.

2. $YbCl_2$ was made by heating $YbCl_3$ and Yb in a molybdenum crucible at a temperature of 850-900°C for 3 hours.

3. $YbCl_3$ was mixed with zinc and heated to produce $YbCl_2$. A 0.5% w.w. oxide contaminate was found.

4. Yb was heated in a stream of H_2 and HCl at 850-900°C. A mixed valence compound, $3YbCl_3 \cdot 5YbCl_2$ resulted.

Corbett (1972)[12] postulated that lanthanide triiodide reacts with an SiO_2 quartz reaction vessel at 800°C by the following equation, $2LnI_3(s) + SiO_2(s) \rightarrow 2LnOI(s) + SiI_4(g)$. Therefore, the suitability of quartz as a reaction vessel for iodides was put into question. A new method[13] for preparing lanthanide trihalide was proposed. In this method, the metal

was allowed to react with an excess of molten mercuric halide in a Pyrex tube at a temperature of 300°C. All trihalides except that of Yb were made. The excess mercuric halide and mercury were removed by sublimation. All metal trihalides were then purified and sublimed in a tantalum container under vacuum.

Corbett (1973)[32] synthesized rare earth trihalides by reaction of the metal with HCl, Br_2 or I_2. Molybdenum boats were used for the chloride synthesis whereas tungsten boats were used for the bromide and iodide syntheses. The rare earth trihalides were distilled and the metal-metal trihalide phase diagram was determined. Both $YbCl_3$-Yb and YbI_3-Yb systems were examined in this study.

A sodium reduction of ytterbium trihalides in HMPA (hexamethyl phosphoramide) at room temperature yielded YbX_2.[18,19] The anhydrous ytterbium trihalides were prepared by the ammonium halide method. All work was done in a dry box filled with argon.

In 1977, the first reaction of ytterbium with 1,2-diiodoethane under an argon atmosphere in a T.H.F. solvent at room temperature was reported.[38] YbI_2 was produced.

In another report, ytterbium metal in T.H.F. is added to the appropriate mercuric halide at room temperature in a Schlenk assembly under dry nitrogen.[22] The ytterbium trihalide produced is extracted in a soxhlet assembly.

The properties of ytterbium 2+ in solutions of HMPA, acetonitrile and ethanol were reported.[35] YbI_2 and $YbCl_2$ were prepared by the following high temperature methods and later dissolved in each solvent. YbI_2 was prepared by the addition of Yb to CuI and $YbCl_3$ was reduced by Yb to $YbCl_2$.

$YbBr_2(THF)_2$ was isolated in 60-80% yield by a method which allowed Yb to react with 1,2-dibromomethane in T.H.F. at room temperature.[23] Also, $YbI_2(THF)_3$ and $YbI_2(CH_3CN)_5$ were isolated by the Yb-diiodoethane synthetic route.

The synthesis of YbI_2 by the action of diiodoalkanes (alkane = methane, butane) on ytterbium metal in T.H.F. in a Schlenk apparatus at room temperature was reported.[25] Dioxan, diethylether, and dimethoxyethane were tried unsuccessfully as other solvents in lieu of T.H.F.

Ytterbium dichloride[26] was obtained by the reduction of the trichloride with hydrogen at 650°C or Yb in a molybdenum or quartz ampoule at 750°C.

Reactions of organolanthanoid[27] compounds are summarized. The synthesized complexes yield $YbCl_2$ or YbI_2 as *undesired* end products.

A study of the kinetics of the oxidation of ytterbium 2+ in aqueous and an aqueous/ethanol solution was reported.[33] The $YbCl_2$ was made by adding 99.9% pure Yb metal to $YbCl_3$ and heating the mixture to 800°C in a molybdenum crucible in an oxygen free argon atmosphere.

The temperature and time dependence of the iodination of ytterbium was studied[29] by reacting metallic Yb with iodine to form YbI_2 and YbI_3. The reaction vessel was quartz which was evacuated to $1x10^{-2}$ torr and cooled in liquid nitrogen. The melting point of YbI_2 was found to be 772 ± 4°C.

The synthetic methods for preparing divalent ytterbium halides vary from:

1. $YbX_3(l) + H_2(g)$(reduction)

   X = Cl [37]

2. $YbX_3(l) + Yb(s)$(reduction)

   X = Cl [11]

3. $YbX_3(s) + Zn(l)$(reduction)

   X = Cl [3]

4. $YbX_3(s)$ + Al,Sn(l)(reduction)

   X = Cl [5]

5. $Yb(s) + X_2(g)$(halogenation)

   X = I [29]

6. Yb(s) + $NH_4X(solv)$ in liq. NH_3(low temperature)

   X = Cl, Br, I [8]

7. $Yb_2O_3(s)$ + HX(aq) + $NH_4X(aq)$ + $ZnX_2(l)$ + $Zn(l)$(reduction)

   X = Cl [10]

8. $YbX_3(s)$ + $Na(s)$ in HMPA(reduction)(room temperature)

   X = Cl, Br, I [18]

9. $Yb(s) + XCH_2CH_2X(s)$ in T.H.F.(room temperature)

   X = I [38]

10. $Yb(s) + CuX(l)$(oxidation)

$X = I$ [35]

The synthetic methods for preparing trivalent ytterbium halides vary from:

1. $Yb_2O_3(s) + X_2(g), HX(aq),$ (halogenation)

$X_2 = Cl_2$ in CCl_4;[1] S_2Cl_2 and Cl_2 [1]

$HX = NH_4Br + HBr$ [2]

$NH_4I + HI$ [2]

$NH_4Cl + HCl$ [2]

2. $Ln(s) + HgX_2(l)$(oxidation)

Ln except Yb; X = Cl, Br, I [4]

Ln = Yb; X(in THF) = Cl, Br, I (room temperature)[22]

3. $YbX_3 \cdot H_2O(s) + HX, NH_4X$(dehydration)

X = Cl, Br, I [1]

4. $YbX_2(s) + X_2(g)$(halogenation)

X = I [4]

5. $Yb(s) + HX(g)$or $X_2(g)$(oxidation)

X = Cl, Br, I [32]

HISTORICAL

X-Ray Diffraction

This section presents a brief chronological review of the papers on x-ray diffraction that concern both ytterbium dihalide and ytterbium mixed halide systems.

The structure of YbI_2 was determined (1960) to be hexagonal with the following lattice parameters: a = 4.503(3) and c = 6.972(4)A[41] The YbI_2 was synthesized by the reaction of Yb with YbI_3 at 550°C under vacuum. Also, YbI_2 prepared by reaction of Yb dissolved in liquid NH_3 with NH_4I was found to exhibit a cubic structure with the following lattice parameter: a = 4.404(2)A[43]

The crystal structure for $YbBr_2$ was reported (1971) to be isostructural[15] with that of $CaCl_2$ with the following lattice parameters: a = 6.63, b = 6.93, and c = 4.37A The same paper states that YbI_2 is isostructural with CdI_2 and $YbCl_2$ is isostructural with SrI_2. The last structure, that of $YbCl_2$, was known (1971) to have the following lattice parameters:[16,40] a = 13.18, b = 6.96, and c = 6.70A

A book[36] on lanthanide, halides, actinide halides and oxide halides describes the $YbCl_2$ structure as a seven coordinate Yb cation with four halogens at the corners of a square and three other halogens at the corners of an equilateral triangle (Figure 1). One of the $YbBr_2$ structures exhibits a distorted rutile type structure with octahedrally coordinated cations. Finally, YbI_2 exhibits a CdI_2 layered structure containing octahedrally coordinated cations (Figure 3).

$YbBr_2$ was found to be polymorphic with an SrI_2 type phase[17] with lattice parameters, a = 13.786, b = 7.358 and c = 7.088Å

Later, $YbBr_2$ was found to exhibit four temperature dependent structure types (1981)[30] as follows: SrI_2 (Figure 1), α-PbO_2 (Figure 2), $CaCl_2$ (Figure 2) and rutile (Figure 4). Lattice parameters for all these structure types were reported.

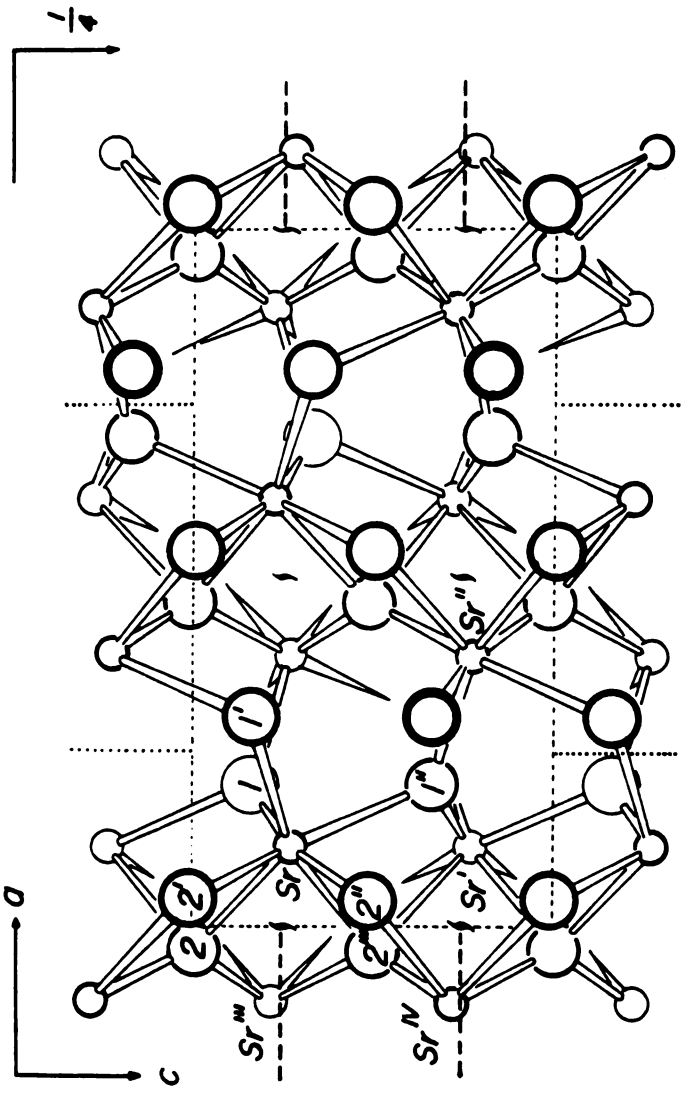

Figure 1. Structure of SrI_2, adapted from reference 48.

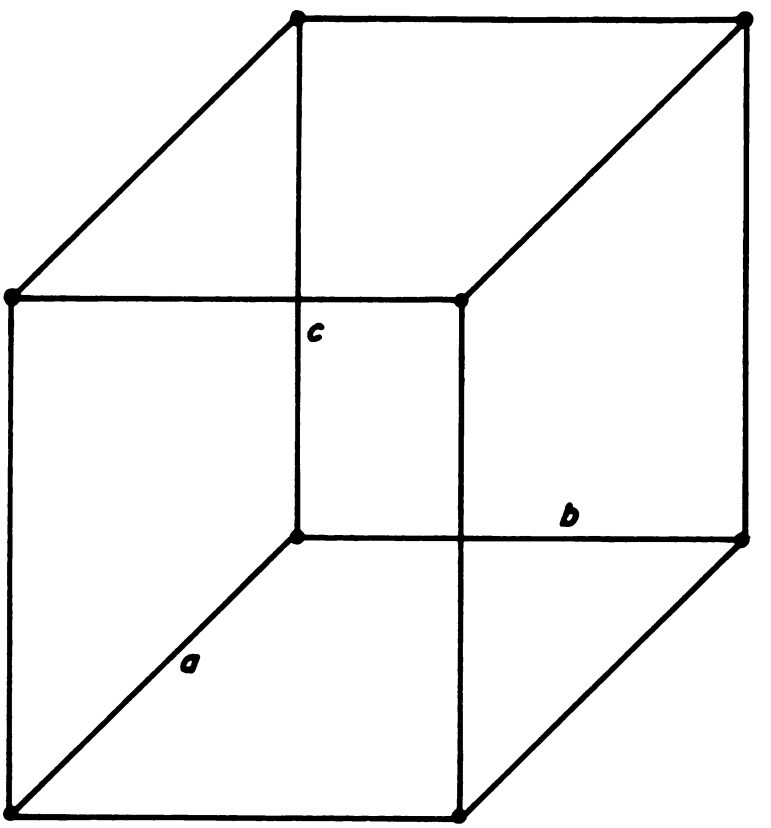

Figure 2. Simple Orthorhombic (P) Bravais lattice with three unequal orthogonal axes indicated. Both α-PbO_2 and $CaCl_2$ structures exhibit this symmetry.

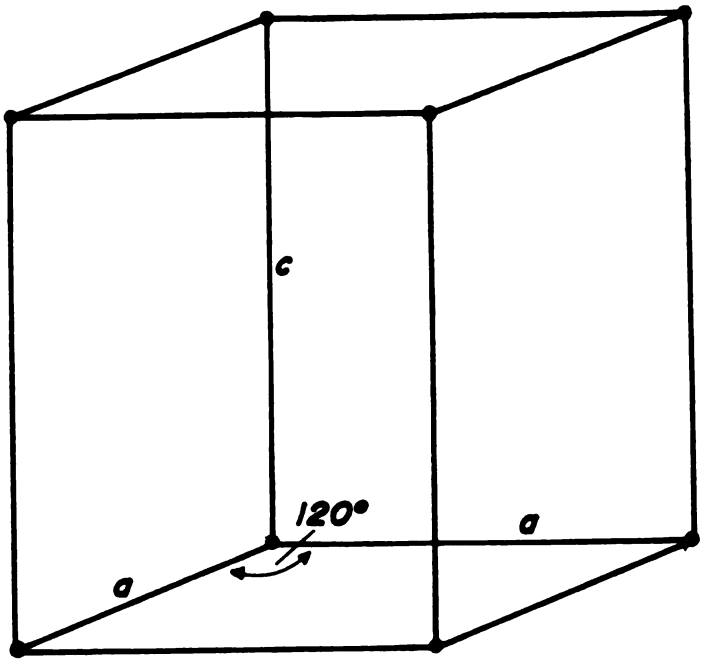

Figure 3. Hexagonal (P) Bravais lattice with cell edges and non-orthogonal angle indicated.

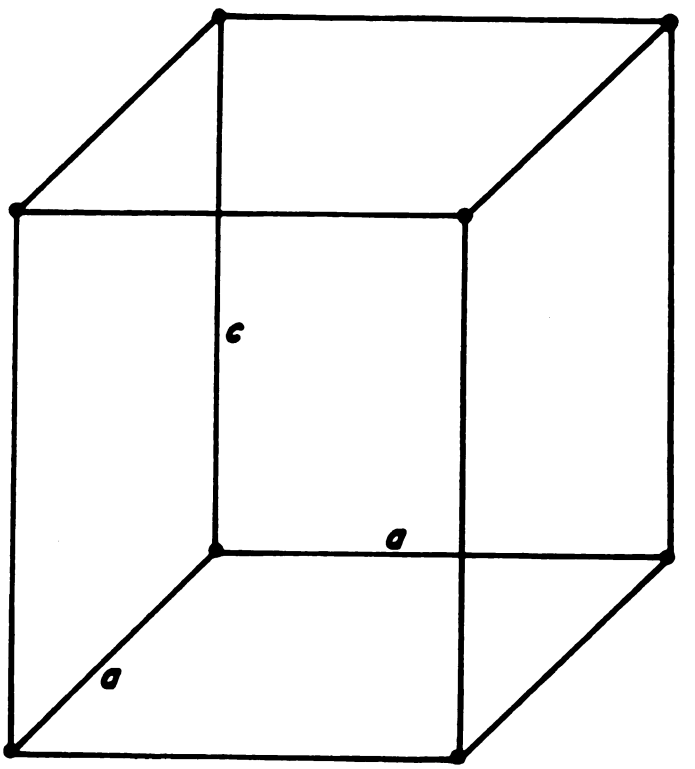

Figure 4. Simple Tetragonal (P) Bravais lattice with orthogonal edges indicated. Rutile (TiO_2) exhibits this symmetry.

EXPERIMENTAL

Reagents

In any synthetic experiment, the percent purity and the impurities of each the reagents used is very important. The reagents selected for this work are listed in Table 1.

Table 1. Reagents Used for Synthetic Work.

Compound or Element	Purity (%)	Impurities (%)	Manufacturer
Ytterbium-Yb (Yb-M$_3$-141D)	99.9	0.03 Mg <0.01 others	Research Chem. Phoenix, AZ.
Ytterbium-Yb (62973)(ultrapure)	99.9	all ppm levels	Research Chem. Phoenix, AZ.
Mercuric Iodide HgI_2	Analytical Reagent Grade	Hg Matter-0.10 Other <0.02	Mallinckrodt St. Louis, MO.
Zinc Chloride $ZnCl_2$	Reagent ACS 97.0	Substance not pptd. $(NH_4)_2S$-0.2 SO_4-0.01 Other < 0.005	Matheson, Coleman & Bell Norwood, OH.
Zinc Bromide $ZnBr_2$(85131)	99.83	No other information	Alfa Products Danvers, MA.
Hydrochloric Acid HCl	ACS electronic grade 36.5-38.0	<0.001	Columbus Chemical Ind. Columbus, WI.
Mercuric Bromide $HgBr_2$	Reagent Grade ACS	Cl-0.25 insol in MeOH-0.05	Matheson, Coleman & Bell Norwood, OH.
Tantalum Ta	unavail.	unavail.	Fansteel N. Chicago, IL.
Mercuric Chloride $HgCl_2$	Certified ACS Grade	Residue after ignition <0.018 Fe 0.0008	Fisher Scientific Fairlawn, NJ.

General Synthetic and X-Ray Equipment

The purity of the reagents and the laboratory equipment are essential parts of a successful synthetic experiment. In this section, the following laboratory equipment will be shown:

Figure 5: Three types of glassware designed for synthesis experiments.

Figure 6: Vacuum apparatus used for synthetic methods.

Figure 7: Induction generator.

Figure 8: Synthetic equipment used for melt experiments.

Figure 9: Glass boat for melt experiments.

Figure 10: Guinier X-ray diffraction instrumentation.

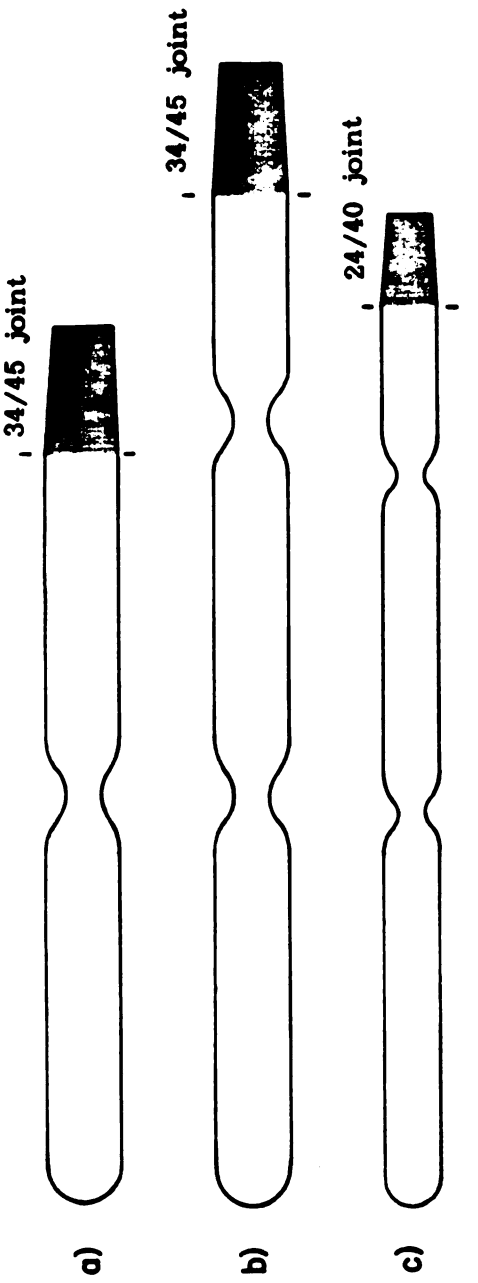

Figure 5. Three types of glassware used in synthesis experiments

a) Pyrex one bulb glass tube
b) Pyrex two bulb glass tube
c) quartz two bulb glass tube

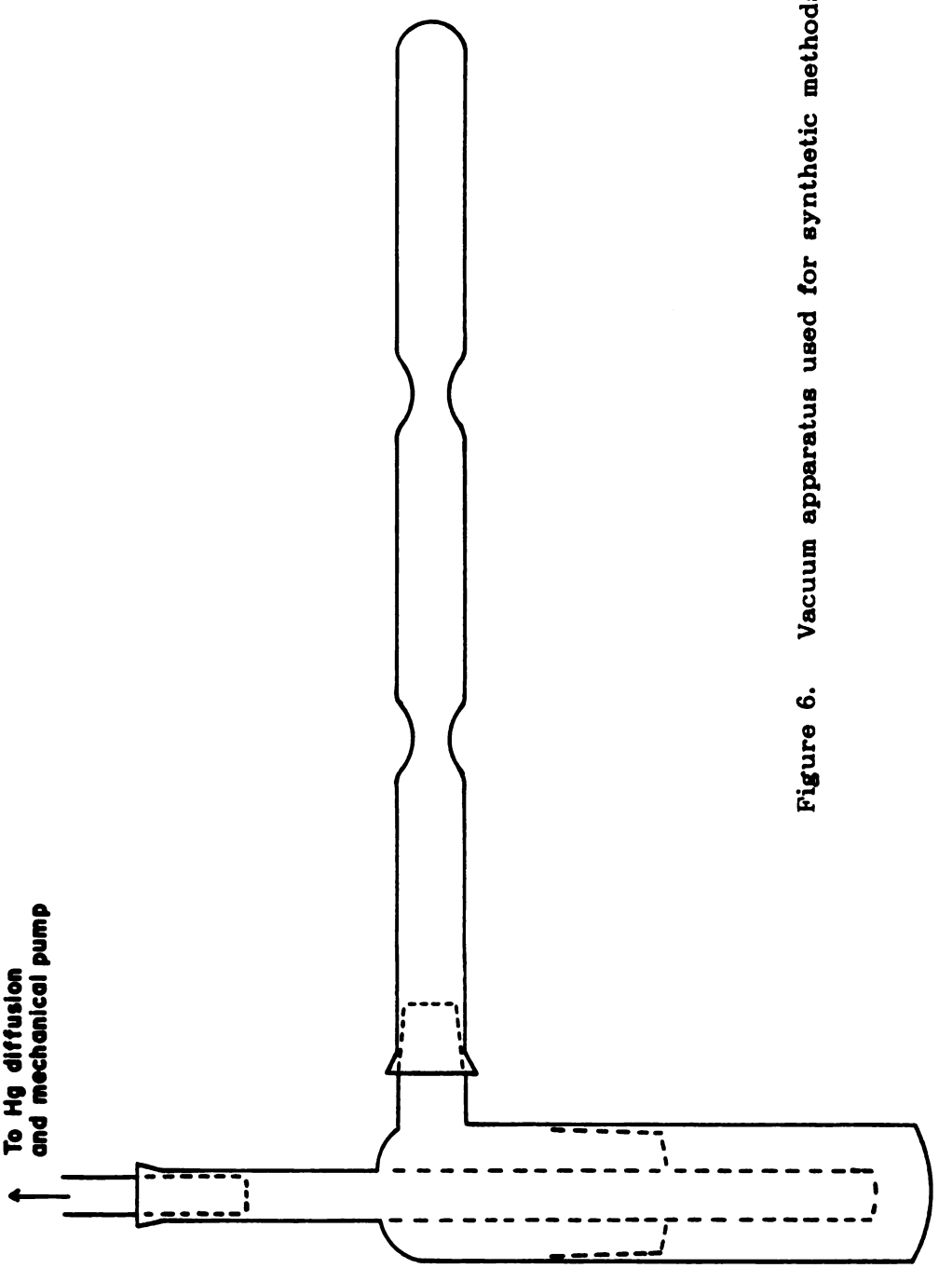

Figure 6. Vacuum apparatus used for synthetic methods.

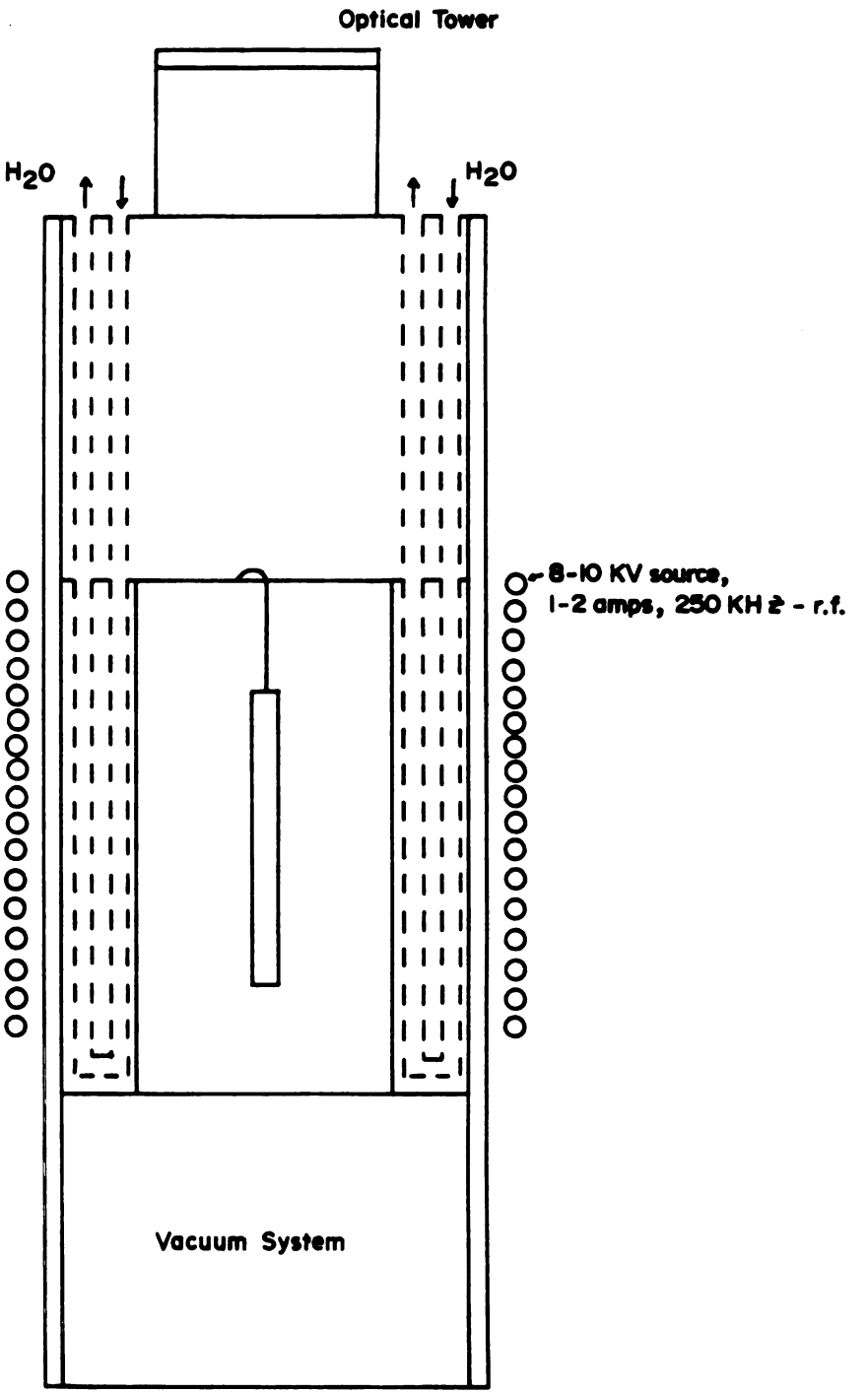

Figure 7. Induction generator for synthesis experiments.

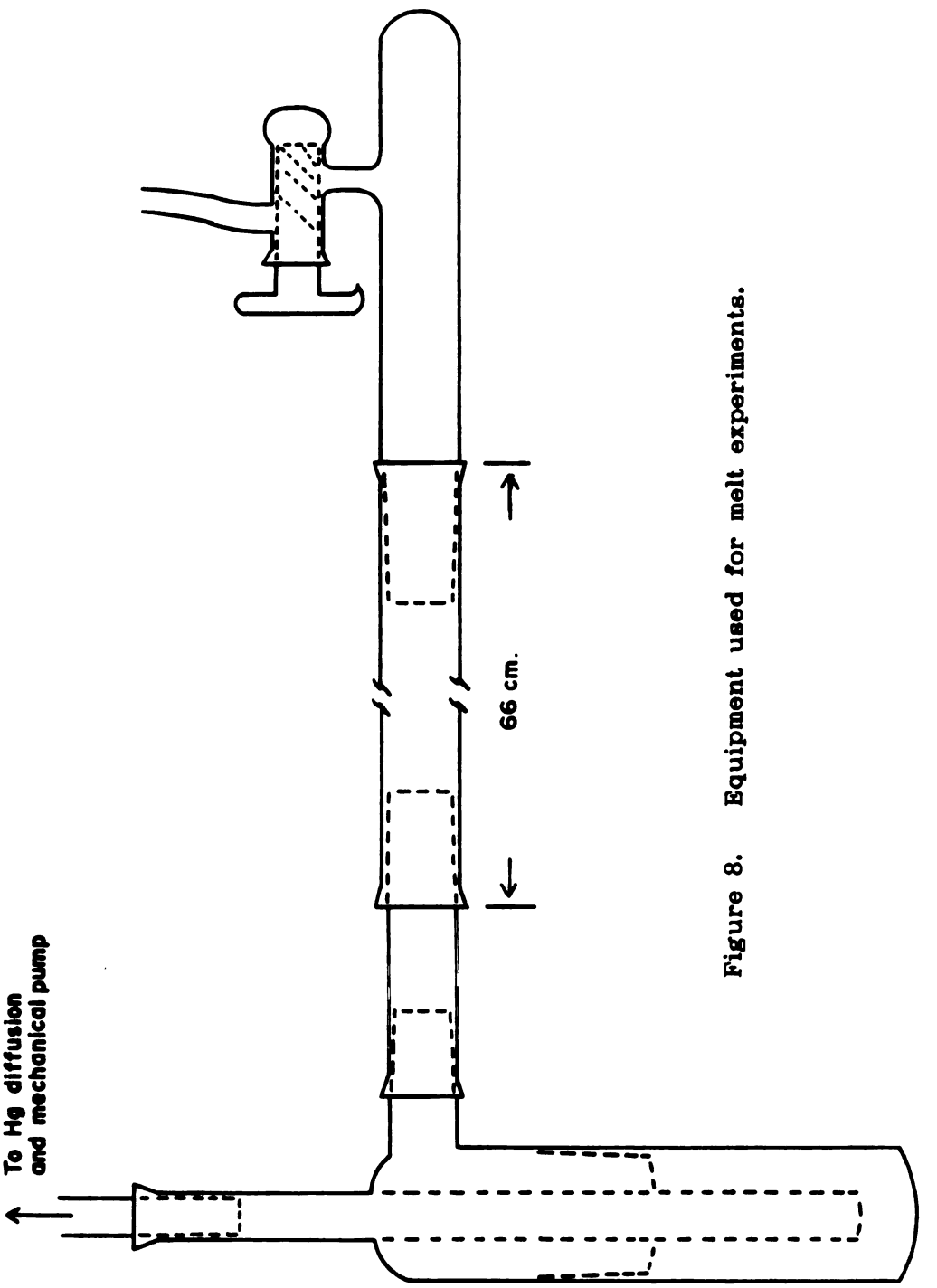

Figure 8. Equipment used for melt experiments.

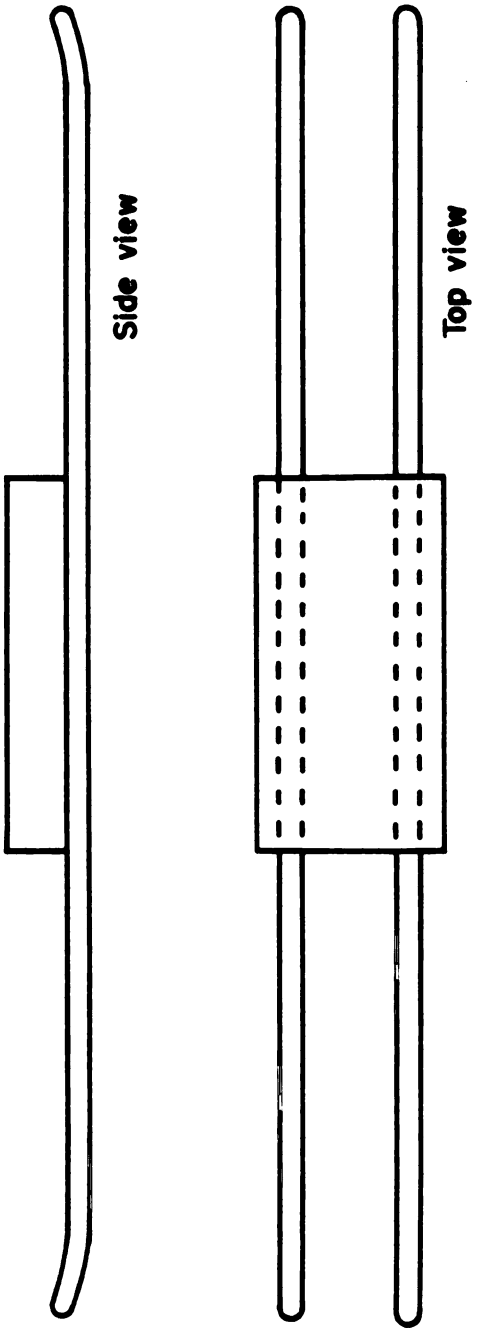

Figure 9. Glass boat used to support and transport melt experiments.

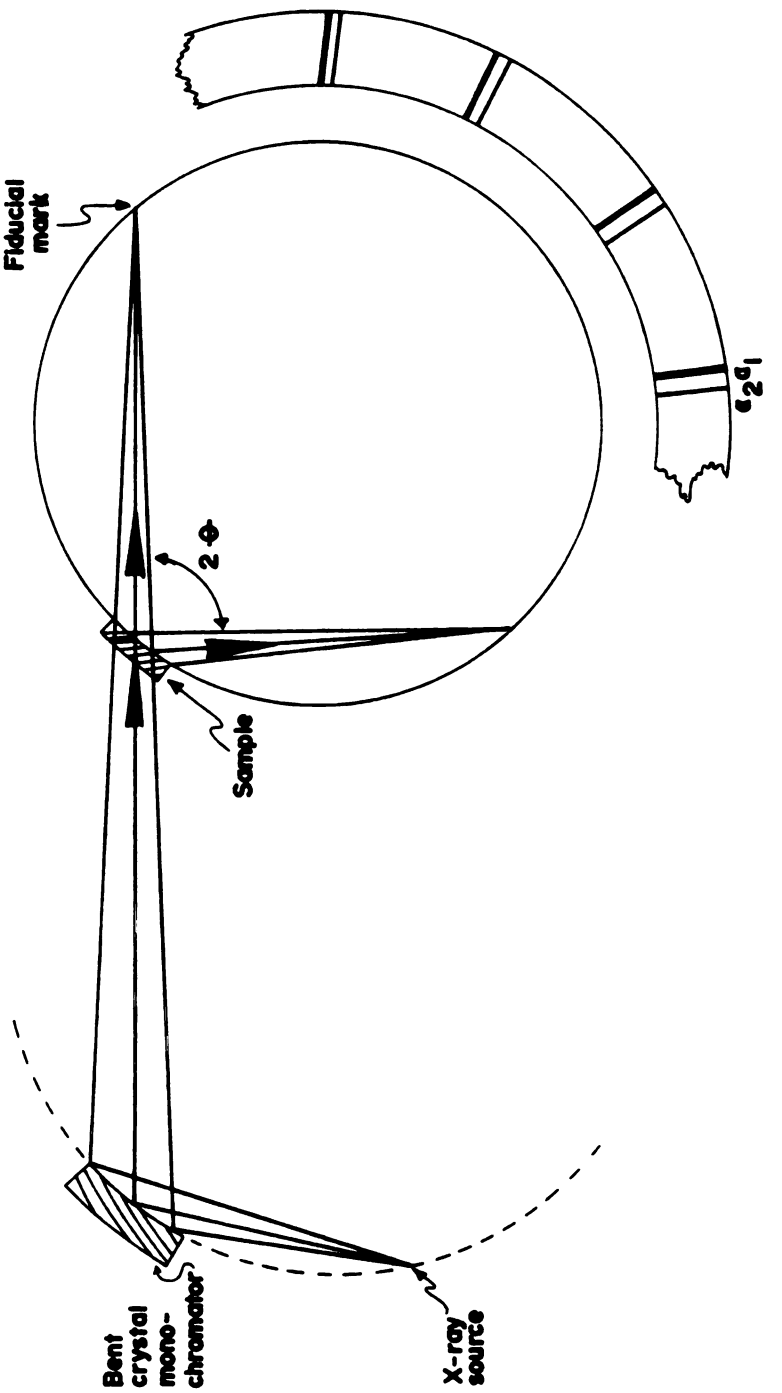

Figure 10. Optics of Guinier X-ray diffraction instrument.

Synthetic Procedures

The first synthesis in which the procedure developed by other laboratories was to be modified was that of $YbCl_2$. In the literature procedure,[10] ytterbium oxide is added to ammonium chloride and zinc chloride in an excess of HCl to yield a matrix of hydrated ytterbium trichloride, NH_4Cl and $ZnCl_2$ as the initial product. This initial mixture is heated in a beaker to dryness to remove excess water and excess hydrochloric acid. The dried mixture is transferred to a quartz tube, and zinc is then added. The quartz tube was evacuated by a mechanical pump and heated to remove the remaining water and excess ammonium chloride. The system was pressurized to one atmosphere with N_2 and the temperature was increased so the zinc chloride and zinc became molten. This molten mixture reacted with the solid $YbCl_3$ to produce $YbCl_2$. Heating at a lower temperature removed excess ammonium chloride and at a higher temperature removed excess zinc and zinc chloride. This procedure takes about one week.

In synthesis number one at MSU, 16.0g (0.12 mole) of $ZnCl_2$ was added to a two bulb Pyrex tube (see Figure 5b) and placed in a horizontal tubular furnace. This Pyrex tube was evacuated by a mechanical pump (see Figure 6) and heated at 340°C until the $ZnCl_2$ melted. By opening the oven, the tube was cooled and later was sealed by a methane/oxygen torch. This sealed tube was placed in another tubular furnace and heated to 450°C for an overnight period to separate any non-volatile (ZnO) impurity. The next morning, 1.5 cm of the tube was pulled out of the furnace. After the $ZnCl_2$ has condensed in the top of the bulb, the tube was cooled and partially cracked by a file mark touched by the methane/oxygen torch. It was immediately placed

in the glove-box. Next, an empty quartz tube (see Figure 5c) was heated under vacuum for two hours at 700°C and cooled. A piece of Parafilm was placed on the tube opening and the tube was immediately put in the glove box. Eight g (0.059 mole) of purified $ZnCl_2$ were added to 2.5 g (0.014 mole) of Yb in the quartz tube in the glove box (060b/84). Parafilm was then placed on the top of the quartz tube, and the tube removed from the glove box. This tube was placed on a vacuum line, evacuated and sealed with a torch. The tube was heated in a furnace at a 45° angle at 550°C for a three day period. The upper part of the tube was gradually pulled out, 1.5 cm at a time until all the $ZnCl_2$ and Zn had condensed in this cooler region. The tube was cooled, scratched with a file and placed in the glove-box. The product ($YbCl_2$?) in the lower bulb was placed in a bottle and stored in the glove-box. The presumed equation for the reaction is:

$$Yb(s) + ZnCl_2(l) \rightarrow YbCl_2(s) + Zn(g)$$

In a second attempt, 10 g (0.073 mole) of $ZnCl_2$ was placed in a two bulb Pyrex tube and heated at 340°C in a tubular furnace for one half an hour. Then, the oven was opened and the tube cooled. The tube was sealed, scratched with a file and placed immediately in the glove-box.

An empty quartz tube was heated at 1000°C in an oven for 3 h while under vacuum. The tube was cooled under vacuum, and parafilm was placed on the top of the tube. Immediately, the tube was placed in the glove-box. In the glove-box, 3.30 g (0.024 mole) of purified $ZnCl_2$ and 2.0 g (0.012 mole) of Yb were added to the quartz tube (068b/84). This tube was placed on a vacuum line, sealed and heated in a tubular furnace overnight at 550°C. Again, the upper part of the tube was

pulled out of the furnace 1.5 cm at a time to effect separation of the Zn and $ZnCl_2$.

The X.R.D. pattern from this synthesis (060b/84) indicated $YbCl_2$ was not pure so an attempt was made to remove the Zn and $ZnCl_2$ impurity. In the glove-box, the $YbCl_2$ complex (075b/84) was placed in a 5.5 cm by 1.8 cm by 0.7 cm pyrolytic graphite boat which was put in a larger glass boat for stability (see Figure 9). These boats were put in a glass tube with a stopcock and a removable top (see Figure 8). This apparatus was connected to a 66 cm by 2.5 cm cylindrical quartz tube which was connected to a vacuum system. Both boats were transferred to the middle of the cylindrical quartz tube and heated to 540°C for 15 min. Excess Zn and $ZnCl_2$ distilled to the colder ends of the quartz tube.

Due to the low two g yield in all previous synthetic preparations of $YbCl_2$, a new synthetic route was tried. This is the proposed equation of the two step reaction:

1. $2Yb(s) + 3HgCl_2(l) \rightarrow 2YbCl_3(s) + 3Hg(g)$

2. $Yb(s) + 2YbCl_3(l) \rightarrow 3YbCl_2(s)$

In step one, 4 g (0.023 mole) of Yb and 40 g (0.15 mole) of $HgCl_2$ (085b/85) were added to a Pyrex two bulb tube. This tube was placed on a vacuum line, sealed and heated in a tubular furnace for three days at 360°C.

Next, 1.1 g (0.0064 mole) of Yb and 3.85 g (0.014 mole) of $YbCl_3$ were added in the glove-box to a 7.6 cm by 0.5 cm tantalum tube (089b/85). The open end of the tantalum tube was crimped shut in the glove-box and both ends were welded under argon or helium. This

welded tube was suspended in the coil region of the induction heating assembly (see Figure 7) and heated at 1000°C for 15 min.

The second synthesis tried was the preparation of $YbBr_2$. Two g (0.012 mole) of Yb and 12 g (0.053 mole) of $ZnBr_2$ were added in the glove-box to a previously heated quartz tube (058a/84). Parafilm was placed on the open top of the quartz tube as a barrier to oxygen and water from the air. Then, the quartz tube was connected vertically to a vacuum line. The tube was evacuated by a mechanical pump and after ten minutes, the system was pressurized with argon to ≈130 torr. The tube was heated with a vertical tubular furnace to 200°C. The temperature of the oven was increased very gradually over a one-day period to 340°C. Then, the sample was heated overnight at 340°C. The sample was cooled and evacuated with a mercury diffusion pump. The temperature was set at 380°C and increased to 500°C over the course of one day. The sample was heated for one week at 500°C to remove excess Zn and $ZnBr_2$.

Then, the quartz tube was cooled and removed to the glove-box. The product was purified further by transferring it to another quartz tube. (Note: all empty quartz tubes were heated for 2 hours at 700°C while under high vacuum.) This tube was sealed under vacuum and heated to 650°C to remove any remaining Zn and $ZnBr_2$ by sublimation to the cooler end of the tube.

The presumed equation is shown below:

1. $Yb(s) + ZnBr_2(l) \rightarrow YbBr_2(s) + Zn(g)$

In the second synthesis (064b/84), the same masses of Yb and $ZnBr_2$ were placed in a two bulb quartz tube. The tube was sealed and put in a tubular furnace which was heated at 400°C for one day. This

sample was placed in a large tubular furnace. The lower bulb was heated at 420°C and the upper bulb at 394°C in order to separate the Zn and $ZnBr_2$ into the upper bulb. Within one day, the temperature of the lower bulb was increased to 500°C and that of the upper bulb to 430°C.

In the next synthetic attempt, 5.2 g (0.23 mole) of $ZnBr_2$ and 2 g (0.012 mole) of Yb were placed in a quartz tube which was evacuated and sealed (068a/84). Then, the quartz tube was heated overnight in a tubular furnace at 550°C. The upper end of the tube was pulled out of the furnace 1.5 cm to separate the Zn which was produced by the reaction. The tube was reheated at a 45° angle at 550°C to remelt the Zn in the upper bulb and allow it to mix with the $YbBr_3$ product in the lower part of the tube. The following equations are suggested:

1. $2Yb(s) + 3ZnBr_2(l) \rightarrow 2YbBr_3(s) + 3Zn(g)$
2. $2YbBr_3(l) + 3Zn(l) \rightarrow 2YbBr_2(s) + ZnBr_2(l) + 2Zn(g)$

Then, the tube was heated at 550°C for one day. The temperature was increased to 580°C to remove the Zn and $ZnBr_2$ and the upper end of the bulb was pulled out of the furnace 1.5 cm at a time to effect separation of the volatile substances by condensation in the upper part of the bulb.

The next $YbBr_2$ synthetic attempt was addition of 2 g (0.012 mole) of Yb and 5.2 g (0.023 mole) of $ZnBr_2$ to a 3.5 cm by 1.5 cm cylindrical Ultra Carbon brand non-pyrolytic graphite crucible which was placed in a quartz tube (070b/84). The empty graphite crucible and the quartz tube had been heated to 800°C for 2 hours. The crucible was placed in a quartz tube and heated in the vertical tube furnace at 550°C for one day under ≈130 torr argon. The quartz tube was then cooled and later

evacuated with the mechanical pump. The temperature was raised over one day to 580°C to remove the Zn and $ZnBr_2$.

For the next synthetic attempt, 2 g (0.012 mole) of Yb and 5.4 g (0.024 mole) $ZnBr_2$ were added to a quartz tube which had been heated empty for 3 hours at 1000°C (073a/84). The quartz tube was evacuated, sealed and heated in a tubular furnace at 550°C for two days. Then, the temperature was set to 540°C and the upper part of the tube was pulled 1.5 cm out of furnace to separate the Zn and $ZnBr_2$ by condensation.

The product of this reaction was purified by the same technique as that used in the $YbCl_2$ synthesis (090a/85). The tubular furnace was preheated to 650°C and set on a 10°C per minute scan rate with a linear temperature programmer. The graphite boat with the sample and the heating tube assembly (see Figure 8) was placed in the heated oven with a dry ice cooled trap arranged to condense any halogen gases that might be evolved. The oven was heated to 780°C and cooled quickly.

The next $YbBr_2$ synthesis was tried in a Pyrex tube by adding 1.98 g (0.11 mole) of Yb and 5.35 g (0.024 mole) of $ZnBr_2$ (076b/84). The tube was evacuated, sealed and heated in a tubular furnace for one day at 400°C. The product was placed in a pyrolytic graphite boat and placed in the heating tube assembly (see Figure 8). The oven was preheated to 540°C and the product was placed in the oven for 10 min to remove the Zn and $ZnBr_2$. The product was further purified by heating it a second time at 780°C.

The next synthetic attempt was the preparation of $YbBr_3$. $YbBr_3$ was reduced by Yb to $YbBr_2$. In a Pyrex tube, 2.5 g (0.014) Yb was added to 32.15 g (0.089 mole) of $HgBr_2$ (076a/84). This tube was

evacuated, sealed and heated in a tubular furnace at 260°C for three days. Then, the upper end of the bulb was pulled out of the furnace 1.5 cm to condense Hg, $HgBr_2$ and Hg_2Br_2.

To a 7.6 cm by 0.5 cm tantalum tube, 5.53 g (0.013 mole) of $YbBr_3$ was added to 1.22 g (0.0071 mole) of Yb (079b/84). The same procedure as that used for the $YbCl_2$ synthesis was followed except that the product was heated in the induction heating assembly (see Figure 7) for 15 min at 1040°C. Later, the product was purified of excess Yb by placing it in a 16.0 cm by 2.5 cm by 1.0 cm pyrolytic graphite boat and heating the boat under high vacuum at 650°C (see Figure 8) (083b and 088a/84). Then, the linear temperature programmer was turned on at a 10°C per minute scan rate and stopped at 750°C. The oven was opened and the product was allowed to cool under vacuum.

The following equations are suggested:

1. $2Yb(s) + 3HgBr_2(l) \rightarrow 2YbBr_3(s) + 3Hg(g)$
2. $Yb(s) + 2YbBr_3(l) \rightarrow 3YbBr_2(s)$

Another synthesis in tantalum was tried with 3.173 g (0.0077 mole) of $YbBr_3$ and 0.68 g (0.0039 mole) of Yb. The induction heating assembly was heated to 960°C for 15 min (12/85).

Finally, the last synthetic route attempted was the preparation of YbI_2. In a Pyrex tube 2.5 g (0.014 mole) of Yb was added to 27 g (0.059 mole) of HgI_2 in air (053b/84). The tube was evacuated, sealed and placed in a tubular furnace at 285°C for three days. Then, the upper part of the bulb was pulled out of the furnace 1.5 cm until all Hg, Hg_2I_2, and HgI_2 had condensed. The cooled Pyrex tube was scratched with a file and transferred quickly into the glove-box. The following equation is suggested:

1. $Yb(s) + HgI_2(l) \rightarrow YbI_2(s) + Hg(g)$

All percent yields were calculated by the following formula:

$$\% \text{ yield} = a/b \cdot/\cdot c/d \times 100$$

a = actual weight of $YbX_2(g)$

b = molecular weight per mole of YbX_2 (g/mole)

c = actual weight of Yb(g)

d = atomic weight per mole of Yb(g/mole).

Procedures for Melt Experiments

In the glove-box appropriate molar quantities of YbX_2-YbX_2' were weighed in 1 g or less quantities. (Note that X and X' represent different halogen atoms.) The two components were ground intimately together in an agate mortar with a pestle to insure homogeneity. The entire sample was placed in a 5.5 cm by 1.8 cm by 0.7 cm pyrolytic graphite boat which was then placed in a large alundum or glass boat (see Figure 9). The apparatus was transferred to a vacuum heating assembly by using a transfer tube with a stopcock and a connecting top (see Figure 8). All glass connections were sealed with an Apiezon grease.

The vacuum heating assembly was evacuated immediately after insertion of the transfer tube. Both boats were transferred to the middle of the 66 cm x 2.5 cm cylindrical quartz tube. The entire heating assembly was subjected to the high vacuum of the mercury diffusion pump. The mixture was heated by a tubular furnace so the temperature exceeded the melting point of at least one of the YbX_2 components (see Tables 2, 3, and 4 for actual temperatures and conditions).

Table 2. Laboratory Data for $YbCl_2$-YbI_2 Melt Experiments.

Mole % $YbCl_2$	Number	Weight of $YbCl_2$	Weight of YbI_2	Initial Temp.	Final Temp.	Time at Final Temp.
10	081b-85	0.052 g	0.800 g	680°C	780°C	5 min
20	078b-84	0.708	0.119	--	800	5
25	073a-84	0.518	0.117	--	800	5
35	084a-85	0.132	0.420	680	780	2
40	083a-85	0.153	0.396	680	780	2
45	080a-85	0.194	0.430	680	780	10
50	070b-84	0.496	0.328	--	780	10
60	085a-85	0.321	0.280	680	780	1
65	081b-85	0.319	0.302	680	795*	1
75	077b-84	0.196	0.348	--	800	10

Note: Scan rate of 25°C/min. from initial temp. to final temp.

*Mistake made.

Table 3. Laboratory Data for $YbBr_2$-$YbCl_2$ Melt Experiments.

Mole % $YbBr_2$	Number	Weight of $YbBr_2$	Weight of $YbCl_2$	Initial Temp.	Final Temp.	Time
25	087a-85	0.130 g	0.302 g	680°C	750°C	1 min
50	086a-85	0.402	0.300	680	750	2
55	089a-85	0.252	0.152	680	750	2
65	087b-85	0.251	0.102	680	750	3
75	086b-85	0.411	0.102	680	750	3
85	089a-85	0.401	0.054	680	750	3
95	092b-85	0.597	0.023	680	750	3
40	054 -85	0.179	0.198	680	750	2

Note: 1. Scan rate of 25°C/min. from initial temp. to final temp.

2. Melts not removed from oven until temp. was 25°C.

Table 4. Laboratory Data for $YbBr_2$-YbI_2 Melt Experiments.

Mole % $YbBr_2$	Number	Weight of $YbBr_2$	Weight of YbI_2	Initial Temp.	Final Temp.	Time
15	095b-85	0.049 g	0.351 g	720°C	750°C	2 min
25	093a-85	0.104	0.402	720	772	2
30	094b-85	0.101	0.302	720	740	1
35	096b-85	0.103	0.249	720	740	1
40	094b-85	0.200	0.403	720	750	2
42	097b-85	0.101	0.182	720	740	1
45	097a-85	0.101	0.158	720	740	1
50	093b-85	0.203	0.248	720	750	2
60	097b-85	0.251	0.209	720	740	1
75	094a-85	0.447	0.197	720	750	1
80	096b-85	0.353	0.113	700	720	1
85	095a-85	0.452	0.104	700	720	1

Note: Scan rate of 25°C/min. from initial temp. to final temp.

The two boats containing the melted specimen were moved from the 66 cm x 2.5 cm cylindrical quartz tube to the transfer tube while the apparatus was under vacuum. The system was removed from high vacuum by turning the stopcock of the mercury diffusion pump in an off position. Then, the system was filled with dried argon, and the transfer tube was removed from the line. The tube was capped quickly and transferred to the glove-box. Each melt was weighed and stored in a one ounce bottle. An X.R.D. pattern was taken.

All percent recoveries were calculated by the following formula:

% recovery = a/b x 100

a = final weight of ytterbium mixed halide(g)

b = initial weight of ytterbium mixed halide(g)

Procedures for X-Ray Diffraction

Interplanar d-spacings and corresponding $\sin^2\theta$ values were obtained from a 100 mm evacuated Guinier-Hagg camera fitted with a quartz monochromator with Cu $K\alpha_1$ x-ray radiation. Samples were placed on Scotch brand tape affixed to metallic donuts and protected from the atmosphere by a film of paraffin oil dried over metallic sodium. The oil was subsequently covered by a very thin piece of glass which was part of a broken glass bubble. The x-ray photographs were calibrated by an internal standard of elemental silicon (a_o = 5.43082 ± 0.00004 Å) which was obtained from the National Bureau of Standards.

Distances between the fiducial mark generated by the direct x-ray beam and the reflections on the photographic film from the Guinier-Hagg camera were determined by a Charles Supper film measuring device modified to permit easier identification of the line position and relative intensities which were estimated visually. Values of d and $\sin^2\theta$ were

calculated by a linear regression program on a Hewlett Packard calculator with the Si reflections as the standard. The d-spacings were indexed (assigned h,k,l's) by comparison to literature data or to the output of program ANIFAC[7] run on the CDC CYBER 750 computer. The program ANIFAC generated the reflection intensities, d-values, $\sin^2\theta$ values and Miller indices, h,k,l, for selected space group from input which consisted of lattice parameter variables (a,b,c,α,β,γ) obtained from the literature or estimated from literature data; atomic position variables of similar compounds which possess the same structure types obtained from the literature, and isotropic thermal parameters. Literature values of isotropic thermal parameters were used when available; when unavailable, they were estimated, with the parameter of the cation typically set at 0.8-1.0 Å^2 and that of the anion 3/2 to 2x this value. Atomic scattering factors were taken with appropriate dispersion correction terms from the "International Tables."[14] Consistent with the geometry of the Guinier camera, absorption terms were not included in the calculations. Lorentz polarization and multiplicity terms were calculated by the program.

Lattice parameters were refined and errors calculated by a linear regression program on a Hewlett Packard Series 80 computer. Lattice parameters were calculated for all molar ratios within a given system, and lattice parameters and volume versus composition were plotted. A linear sloping line was considered indicative of a solid solution whereas a line of zero slope was considered indicative of the presence of a new phase. Determination of whether anion site occupancy of mixed halides was random or ordered was effected with the aid of the program

ANIFAC. Calculated intensity data for selected reflections were compared with those determined from a Philips diffractometer (Cu Kα radiation).

RESULTS

Synthetic

The percent yields for syntheses of $YbCl_2$, $YbCl_3$, YbI_2, $YbBr_2$ and $YbBr_3$ are reported in Tables 5 and 6. Percent recoveries for the ytterbium chloride-iodide, bromide-chloride and bromide-iodide systems are tabulated, respectively, in Tables 7, 8 and 9. In Table 10, the x-ray reflections and their intensities calculated or reported for ytterbium oxide halides are tabulated together with reflections observed in the compounds; $YbCl_2$, YbI_2 and $YbBr_2$. These compounds potentially might contain oxide halide impurities.

Table 5. Percent Yields of $YbCl_2$, $YbCl_3$ and YbI_2

Compound	Number	% Yield	Color
$YbCl_2$ [b]	060b-84	24.9	grey/white
$YbCl_2$ [b]	068b-84	40.1	grey/white
$YbCl_2$ [b]	071a-84	74.7	grey/white
$YbCl_2$ [b]	075b-85	90.8	grey/white
$YbCl_2$ [c]	089b-85	a	yellow
$YbCl_3$ [d]	085b-85	90.5	white
YbI_2 [e]	053b-84	92.7	green
YbI_2 [e]	082a-85	85.3	green
YbI_2 [e]	057b-84	96.2	green

a. X.R.D. indicated $YbCl_3$-$YbCl_2$ mixture.

b. $Yb(s) + ZnCl_2(l) \rightarrow YbCl_2(s) + Zn(g)$.

c. $Yb(s) + 2YbCl_3(l) \rightarrow 3YbCl_2(s)$.

d. $2Yb(s) + 3HgCl_2(l) \rightarrow 2YbCl_3(s) + 3Hg(g)$.

e. $Yb(s) + HgI_2(l) \rightarrow YbI_2(s) + Hg(g)$.

Table 6. Percent Yields of $YbBr_2$ and $YbBr_3$

Compound	Number	% Yield	Color
$YbBr_2$ [c]	058a-84	96.5	black/green
$YbBr_2$ [c]	064b-84	55.9	yellow
$YbBr_2$ [c]	068a-84	67.7	yellow/green
$YbBr_2$ [c]	070b-84	none[a]	---
$YbBr_2$(step 1)[c]	073a-84	90.8	yellow/grey
$YbBr_2$(step 2)	090a-85	70.8	green
$YbBr_2$(step 2)[c]	076b-84	21.0	green/white
$YbBr_2$(step 1)[d]	079b-84-E	91.9	red
$YbBr_2$(step 2)	083b-84	none[b]	black/green
$YbBr_2$(step 2)	088a-84	36.9	green
$YbBr_2$(step 1)[d]	091a-84-E	54.6	green
$YbBr_2$(step 2)	091a-84	41.7	black
$YbBr_2$ [d]	146-10-85	93.9	green
$YbBr_2$ [d]	12-85-E	95.6	green
$YbBr_3$ [e]	076a-84	97.4	green/white

a. $YbBr_2$ was absorbed into graphite cylindrical crucible.

b. $YbBr_2$ adhered to the boat.

c. $Yb(s) + ZnBr_2(l) \rightarrow YbBr_2(s) + Zn(g)$.

d. $Yb(s) + 2YbBr_3(l) \rightarrow 3YbBr_2(s)$.

e. $2Yb(s) + 3HgBr_2(l) \rightarrow 2YbBr_3(s) + 3Hg(g)$.

Table 7. Percent Recovery - Ytterbium Chloride/Iodide System.

Mole % $YbCl_2$	Number	% Recovery	Color of Melt
10	081b-85	a	green/black/yellow
20	078b-84	65.8	green/black
25	073a-84	65.2	black/yellow
35	084a-85	70.0	green/black
40	083a-85	48.8	green/black
45	080a-85	81.3	green/black/yellow
50	070b-84	66.6	green/black
60	085a-85	66.7	green/black
65	081b-85	78.3	green/black
75	077b-84	b	green/black

a. No yield reported.

b. Melt difficult to remove from boat.

Table 8. Percent Recovery - Ytterbium Bromide/Chloride System

Mole % $YbBr_2$	Number	% Recovery
25	087a-85	84.7
40	054-75 (book 2)	81.2
50	086a-85	87.7
55	089a-85	66.3
65	087b-85	51.0
65	092b-85	75.4
75	086b-85	65.3
85	089a-85	67.9
95	095b-85	71.9

Table 9. Percent Recovery - Ytterbium Bromide/Iodide System

Mole % $YbBr_2$	Number	% Recovery	Color of Melt
15	095b-85	53.0	black/yellow
25	093a-85	73.5	black/yellow
30	094b-85	74.2	black/yellow
35	096b-85	76.7	black/yellow
40	096b-85	59.9	black/yellow
42	097b-85	76.3	black/yellow
45	097a-85	62.9	black/yellow
50	093b-85	59.0	black/green
60	097b-85	80.7	black/yellow
75	094a-85	72.4	black/green
80	096b-85	62.0	black/green
85	095a-85	73.7	black/green

Table 10. A comparison of ytterbium dihalides to respective ytterbium oxide halides in terms of d-spacings and intensities of X.R.D. patterns.

		Observed		Calculated	
Compound	Number	d	i	d[a]	i
$YbCl_2$	068b-84	9.3088	W-	9.2767	96.4
		---	---	3.2053	32.0
		---	---	2.9273	100.0
		---	---	2.3658	39.4
		---	---	1.8630	33.1
		d	i	d[b]	i
YbI_2	053b-84	3.0082	W-	2.963	100
		2.7228	W	2.737	55
		---	---	2.409	25
		under Si	---	1.938	40
		1.6177	W	1.622	65
		1.3786	W	1.372	30
$YbBr_2$	083b-85	d	i	d[c]	i
		---	---	2.80	100
		---	---	2.67	100
		1.8922	W	1.89	60
		1.563	W	1.57	60

$YbBr_2$	064b-84	d	i	d^c	i
		2.79919	M	2.80	100
		2.67735	M	2.67	100
		d	---	---	---
		d	---	---	---

a. Intensity and d spacing from computer progran ANIFAC for YbOCl; l.p.-ref. 50; a.p.-ref 50.

b. Intensity and d spacing - ref. 44; 16-60-YbOI.

c. Intensity and d spacing-ref. 44; 12-1465-YbOBr.

d. d values not read.

X-Ray Diffraction

A summary of the SrI_2-type orthorhombic lattice parameters for $YbCl_2$, $YbBr_2$ and the $YbCl_2/YbBr_2$ mixed halide system and respective unit cell volumes are presented in Table 11. A graphic presentation of lattice parameters and unit cell volumes for this system is plotted in Figure 11. Lattice parameters and volumes are given in Table 12 for the hexagonal, CdI_2 structure type observed for part of the $YbCl_2/YbI_2$ system. Data on another portion of this system indexed as the orthorhombic, SrI_2 structure type is presented in Table 13. These lattice parameters and the respective unit cell volumes to which they correspond are displayed graphically in Figure 14.

In the $YbBr_2/YbI_2$ system, the hexagonal CdI_2 type structure was found in the 0 and 35 mole percent $YbBr_2$ samples. In contrast, the orthorhombic, $CaCl_2$ structure type which is one of four structure types reported for $YbBr_2$ was observed in the 80, 85 and 100 mole percent $YbBr_2$ samples. This result is also given in Table 14. Structure types

which were considered in an attempt to identify unexplained reflections in $YbCl_2/YbBr_2$ system are exhibited in Table 15. Attempts were also made to fit the new phase reflections observed in the $YbCl_2/YbI_2$ system to known structure types. These structure types are listed in Table 16.

Table 11. Lattice parameter composition data for the orthohombic SrI_2-type structure, $YbCl_2/YbBr_2$ system. The standard deviation of the least significant digit is indicated in parentheses.

Mole % $YbBr_2$	a	b	c	volume
0	13.158(6)A	6.960(3)A	6.708(3)A	614.18A^3
25	13.316(8)	7.045(5)	6.759(8)	634.07
40	13.52(1)	7.116(5)	6.809(4)	654.41
55	13.547(9)	7.178(5)	6.882(5)	669.16
65	13.579(9)	7.213(5)	6.944(6)	679.94
75	13.630(9)	7.255(4)	6.998(5)	691.85
85	13.71(1)	7.330(7)	7.063(5)	709.59
95	13.764(7)	7.336(5)	7.073(4)	714.08
100	13.80(1)	7.359(4)	7.093(4)	720.12

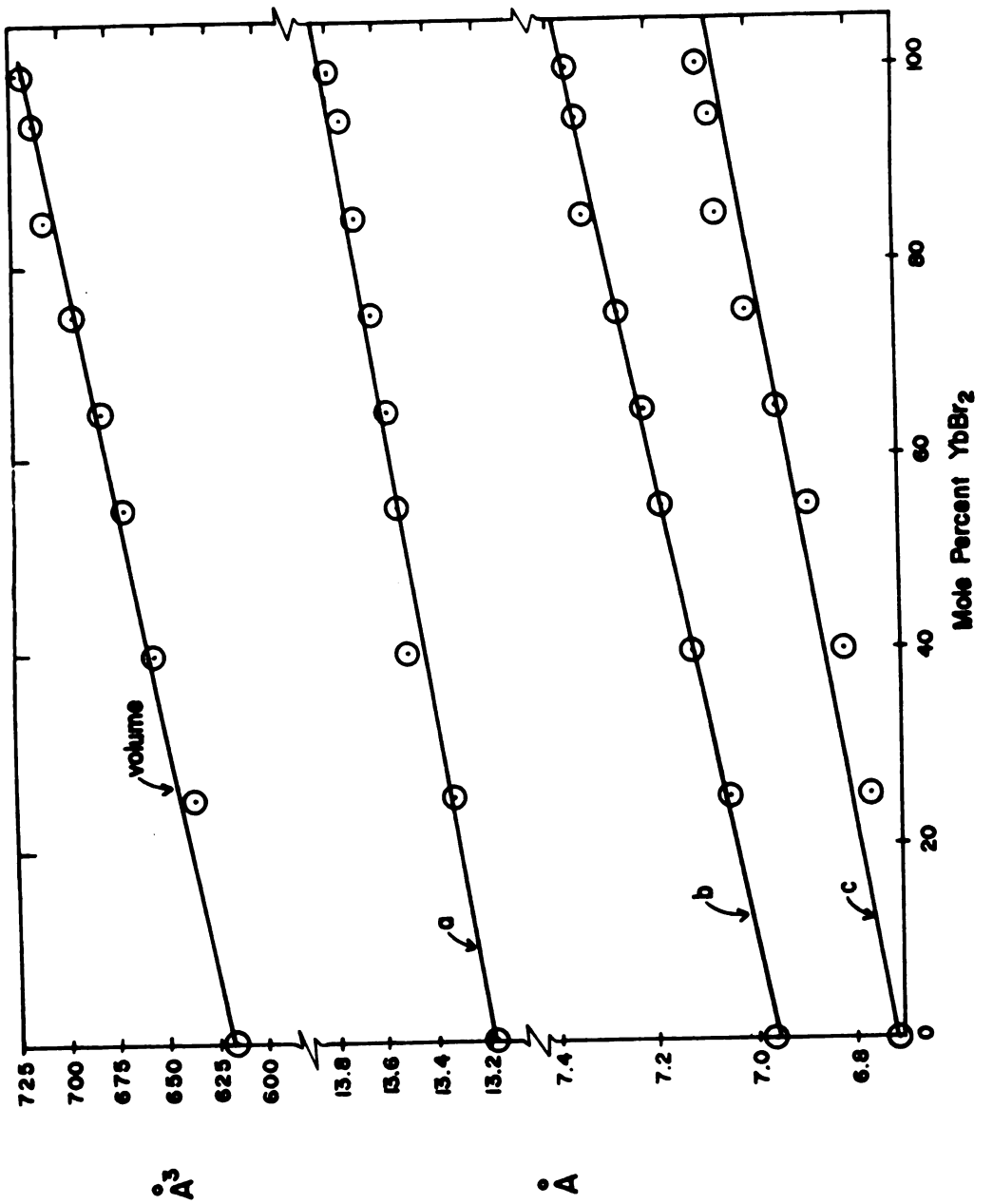

Figure 11. A plot of the orthorhombic lattice parameters and unit cell volume observed in the $YbBr_2/YbCl_2$ system as a function of composition.

Table 12. Lattice parameter composition data for the hexagonal CdI_2-type structure, $YbCl_2/YbI_2$ system. The standard deviation of the least significant digit is given in parentheses.

Mole % $YbCl_2$	a	c	Volume
0	4.508(3)Å	6.978(3)Å	122.74Å^3
10	4.485(6)	6.967(9)	121.37
20	4.451(5)	6.955(7)	119.27
25	4.442(5)	6.949(8)	118.73
35	4.450(6)	6.953(8)	119.17
40	4.451(6)	6.957(9)	119.29
45	4.450(7)	6.95(1)	119.14
50	4.46(3)	6.96(4)	119.73

Table 13. Lattice parameter composition data for the orthorhombic SrI_2-type structure, $YbCl_2/YbI_2$ system. The standard deviation of the least significant digit is given in parentheses.

Mole % $YbCl_2$	a	b	c	Volume
100	13.158(6)Å	6.960(3)Å	6.708(3)Å	614.18Å^3
75	13.175(5)	6.956(3)	6.702(4)	614.07
65	13.182(8)	6.960(4)	6.711(6)	615.57
60	13.18(2)	6.955(7)	6.71(1)	613.70
50	13.11(4)	6.94(2)	6.68(2)	606.86

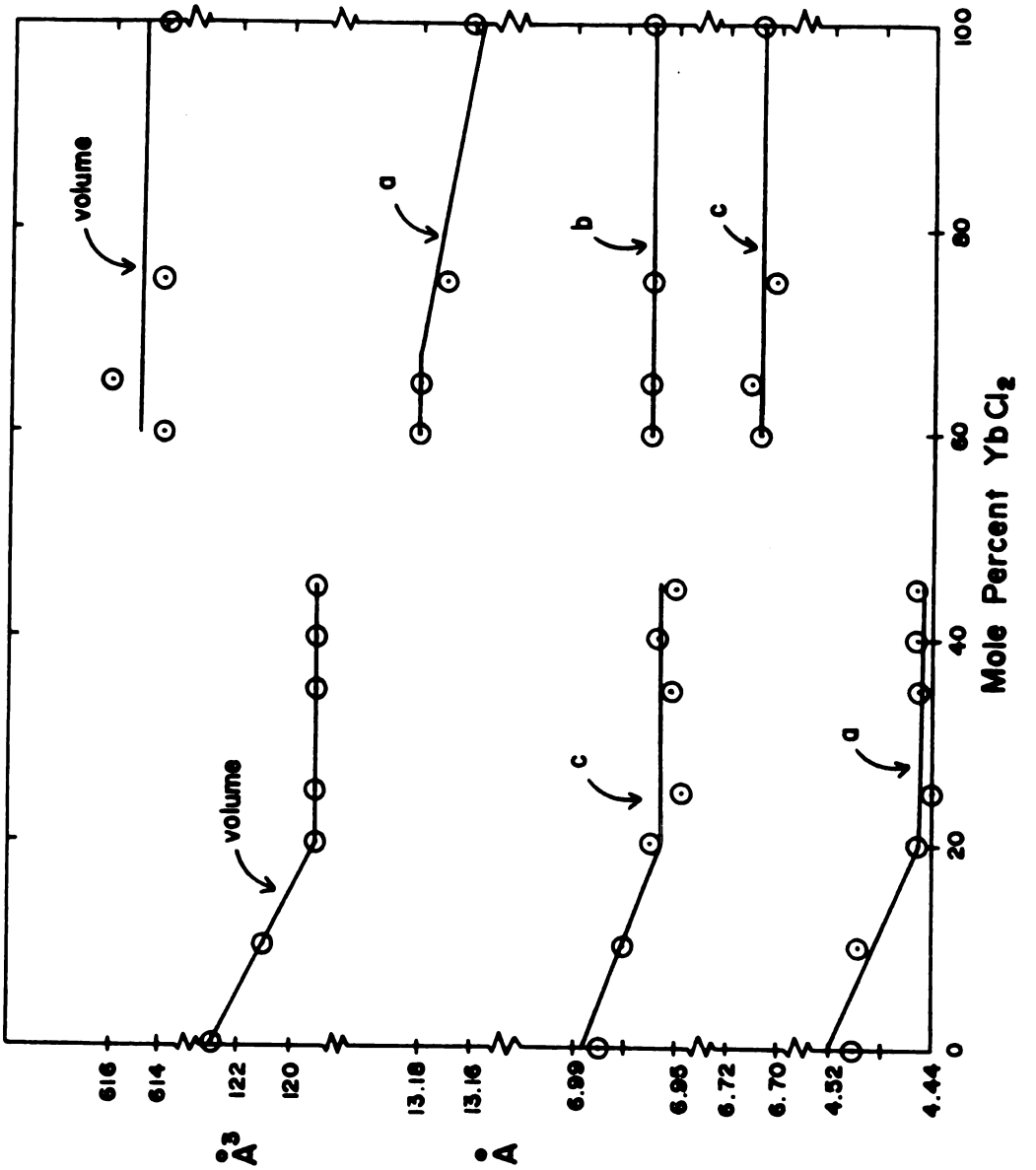

Figure 12. A plot of orthorhombic and hexagonal lattice parameters, together with the unit cell volume observed in the $YbCl_3/YbI_3$ system.

Table 14. Lattice parameter composition data for the hexagonal CdI_2-type structure and orthorhombic $CaCl_2$ type structure, $YbBr_2/YbI_2$ system. The standard deviation of the least significant digit is given in parentheses.

Mole % $YbBr_2$	a	b	c	Volume
0	4.508(3)A	---	6.978(3)A	122.74A^3
35	4.457(5)	---	6.901(7)	118.72
80	6.708(4)	7.019(5)A	4.408(2)	207.54
85	6.680(4)	7.001(5)	4.401(3)	205.82
100	6.6320	6.9320	4.3720	200.99

Table 15. Structure types examined in an attempt to index unexplained reflections in the $YbBr_2/YbCl_2$ system.

1. Rutile[30]

2. $CaCl_2$ [30,15]

3. α-PbO_2 [30]

4. YbOBr [44]

5. YbOCl [50]

Table 16. Structure types examined in an attempt to assign reflections of the new phase observed in the $YbCl_2/YbI_2$ system.

1. $CaCl_2$ [15,30]

2. α-PbO_2 [30]

3. $PbCl_2$ - high pressure form [60]

4. $PbCl_2$ [62]

5. $CdCl_2$ [56]

6. Rutile [30,56]

7. YbOBr [44]

8. PbClF[44]

9. SrI_2 [17,48]

10. YbOI [44]

11. YbOCl [50]

12. SrI_2 (II)[60]

13. CdI_2 [47,64]

14. BiSI [56]

DISCUSSION

Synthetic

In any synthesis, obstacles that inhibit progress appear. Following is a summary of the problems encountered in this work:

1. $YbCl_2$ synthesis method 1: removal of Zn and $ZnCl_2$.

2. $YbCl_2$ synthesis method 2: formation of a $YbCl_3$-$YbCl_2$-$TaCl_x$ mixture.

3. YbI_2 synthesis: Possible formation of $YbI_2 \cdot$ hydrate.

4. $YbBr_2$ synthesis method 1: YbOBr impurity, and a complex X.R.D. pattern due to four known temperature dependent structure types for $YbBr_2$.

5. $YbBr_2$ synthesis method 2: formation of a $YbBr_3$-$YbBr_2$-$TaBr_x$ mixture.

6. Mixed halide systems: low recoveries.

All six problems will be discussed in this section. The first five problems are concerned with impurities in ytterbium dihalide syntheses. All impurities had to be removed before these materials could be used as reactants for the mixed halide studies. Problem six deals with the mixed halide systems. In the $YbCl_2$ synthesis by method one [$Yb(s) + ZnCl_2(l) \rightarrow YbCl_2(s) + Zn(g)$], Zn and excess $ZnCl_2$ proved difficult to separate at 550°C from $YbCl_2$ by the method of choice, sublimation. The vapor pressures of the individual components are a key factor in the sublimation process, and are: $ZnCl_2$ - 40 torr[52] at 566°C, Zn - 10 torr[52] at 593°C and $YbCl_2$ - 2.6×10^{-9} torr[53] at 550°C. Since the sublimation occurred at a temperature of 550°C, the Zn and $ZnCl_2$ should have been

removed easily from the desired $YbCl_2$ product based on vapor pressure factors.

X-ray diffraction results showed $YbCl_2$ and other unidentified compounds to be present in the lower part of the quartz bulb (060b/84). The upper bulb contained both a brown solid ($YbCl_2$ and other unidentified compounds), and a white solid (no $YbCl_2$, but other unidentified compounds).

Raoult's law considerations can provide an explanation for the presence of unidentified compounds, probably Zn and $ZnCl_2$ in the lower bulb. In this case, an ideal solution of Zn, $ZnCl_2$ and $YbCl_2$ is assumed. The law states that the total vapor pressure is the sum of the vapor pressures of each individual component. As such, $P_{total} = P_{Zn} + P_{ZnCl_2} + P_{YbCl_2}$, where $P_{Zn} = X_{Zn}P^{o}_{Zn}$ (P^{o}_{Zn} = vapor pressure of pure Zn, X_{Zn} = mole fraction of Zn, etc.). As the number of moles of zinc approaches zero, the absolute vapor pressure of zinc in the lower bulb approaches that of $YbCl_2$ and zinc ceases to be transported from the lower to the upper bulb at a reasonable rate. The same argument holds for transport of $ZnCl_2$. Therefore, some amount of all three reactants, Zn, $ZnCl_2$ and $YbCl_2$ is contained in the lower bulb.

The reaction time for the next $YbCl_2$ synthesis (068b-84) was reduced from three days to overnight to accelerate the overall synthetic procedure. The sublimation time for removal of Zn and $ZnCl_2$ was reduced from three days to one day in an attempt to minimize transport of $YbCl_2$ to the upper bulb. X-ray diffraction data indicated the presence of $YbCl_2$ in lower bulb, but the yield was low (40.1%). This lower yield is apparently due to transport of $YbCl_2$ to the upper bulb and adhesion of $YbCl_2$ to walls of quartz tube. Apparently, the $YbCl_2$

was transported into the upper bulb along with Zn and $ZnCl_2$. This is due to the high transport rate of Zn and $ZnCl_2$ caused by experimental conditions. This hypothesis is given more validity by the results in the next synthesis in which a larger surface area graphite boat cleanly separated Zn and $ZnCl_2$ from $YbCl_2$.

In the $YbCl_2$ synthesis (071a/84), sublimation time was reduced further to one hour, and the Zn complex was only partially removed. Complete removal of the $ZnCl_2$ and Zn was completed in ten minutes at a temperature of 540°C. The sample was placed in a medium sized graphite boat and placed in a vacuum heating assembly (see Figure 8). A 90.8% yield was achieved on the last $YbCl_2$ synthetic attempt (075b-84).

The products of $YbCl_2$ synthesis (089b/85) by method two, [Yb(s) + $2YbCl_3(l) \rightarrow 3YbCl_2(s)$], were analyzed by X.R.D. and found to be a $YbCl_3$-$YbCl_2$-$TaCl_x$ mixture. A possible explanation is reaction between $YbCl_3$ and the tantalum tube. This reaction apparently produced a $TaCl_x$ compound which expanded the tantalum tube. This expansion was undoubtedly due to the fact that $TaCl_5$ can only exist as a gas[54] at 1000°C. In a thesis written by one of Baernighausen's students,[30] $TaBr_5$ and $TaBr_{2.8}$ were confirmed by chemical tests to be present in the reaction product formed between $YbBr_3$ and a tantalum container. The following equation is suggested for formation of the $YbCl_3$-$YbCl_2$-$TaCl_x$ mixture:

1. $Ta + YbCl_3 \rightarrow TaCl_x + YbCl_2$

Yb metal was also found in the tantalum tube which might suggest the following equation:

2. $Ta + YbCl_2 \rightarrow TaCl_x + Yb(s)$

Alternately, since the $YbCl_3$ and Yb were mixed in the stoichiometric ratio required to produce $YbCl_2$, any $YbCl_3$ that reacted with Ta would of necessity require that Yb metal remain in the reaction tube. This latter explanation (equation 1) seems thermodynamically more feasible than equation 2. No YbOCl was found in any $YbCl_2$ preparation (see Table 10).

In the YbI_2 synthesis, the yields were high due to the high vapor pressure of the following reagents: HgI_2 - 100 torr[52] at 261.8°C; and Hg - 100 torr[52] at 261.7°C. Another possible product, Hg_2I_2 decomposes at 357°C. The vapor pressure of YbI_2 is 1.9×10^{-16} torr[57] at a temperature of 260°C which was calculated from a ΔH° of EuI_2, and vapor pressure of YbI_2 of 2 torr at 790°C.[45] These large vapor pressure differences allowed a clean separation of YbI_2 from Hg and HgI_2 by the sublimation process and according to LeChatelier's principle, forced the reaction to completion. Consequently, all the YbI_2 synthesis yields were high. The less than 100% yield observed could be the result of two causes: (1) the transport of YbI_2 to the upper bulb as mentioned in $YbCl_2$ synthesis discussion, and (2) incomplete reaction if the metal particles were too large to have reacted completely with HgI_2 before the end of the tube was pulled from the furnace and the HgI_2 removed. The major problem with the YbI_2 synthesis was the presence of unexplained reflections in the X.R.D. pattern. The following approaches were taken to identify the unexplained reflections:

(1) YbI_2 is know to exhibit the CdI_2 structure type which forms polytypes[47] in which the cell dimensions vary only in the direction perpendicular to the stacked layers. To approximate polytype 4H by computer, the a^{11} lattice parameter calculated from the X.R.D. pattern of an MSU synthetic preparation of YbI_2 was combined with the doubled c lattice parameter of the same material. Interplanar d-spacings generated by the computer from these parameters did

not match the unexplained reflections in X.R.D. pattern of the MSU preparation of YbI_2. The polytype 6H was also approximated by computer by tripling the c lattice parameter. This computer calculation of interplanar d-values was not the solution either. On the assumption that the reflections were superstructure reflections of the parent cell, an attempt was made to fit them by the method of ITO[58] to a new larger cell. They could not be fit.

(2) Potential impurities were checked by comparison of observed d values with those from the ASTM Powder Diffraction File.[44] Reflections for the following compounds did not match the unexplained reflections:

a) YbOI

b) HgI_2

c) Yb

d) Hg_2I_2

e) Hg

A possible solution was found when an X.R.D. pattern of a 50 mole percent $YbCl_2$-50 mole percent YbI_2 sample, which had been confined in the glove-box for many months, was examined. The YbI_2 reflections found in the original 50/50 $YbCl_2$-YbI_2 X.R.D. film were absent in the rerun and the unexplained reflections were more intense. It is possible that the YbI_2 in the 50/50 $YbCl_2$-YbI_2 rerun could have formed a hydrate or could have oxidized. However, no YbOI was present in the 50/50 YbI_2-$YbCl_2$ rerun. Therefore, it was assumed that the reflections belong to a YbI_2·hydrate, and this assumption was pursued by experimental methods. In the glove-box, 0.1 g of YbI_2 was weighed into a 2 ml reacti-vial. The top was sealed with a Teflon® septum and capped. The vial was removed from the glove-box and 5 microliter of deionized water was injected by a 10 microliter syringe. Then, the vial was placed in the glove-box and an X.R.D. pattern taken. The observed d values of this X.R.D. pattern called the YbI_2·hydrate were identical to

those of the unexplained reflections of the 50/50 $YbCl_2$-YbI_2 rerun. No YbI_2 was present in YbI_2·hydrate or the 50/50 $YbCl_2/YbI_2$ rerun. Ytterbium iodide hydrate compounds have not been reported, so no d values against which to make comparisons are available in the literature. No YbOI was found in any YbI_2 product (see Table 10). In Table 10, the first two observed reflections in YbI_2 (053b-84) were confirmed to be $YbI_2{\cdot}(H_2O)_x$ and the last two d reflections are identified as YbI_2. Even though the reflections observed in the YbI_2 product (053b-84) matched the theoretical YbOI d values, the intensities of these reflections do not match calculated values. Therefore, YbOI is not present.

A major problem with $YbBr_2$ synthesis method 1, [Yb(s) + $ZnBr_2$(l) → $YbBr_2$(s) + Zn(g)], was a YbOBr impurity (see Table 10-064b/84). The following steps were followed in an effort to eliminate YbOBr formation:

(1) The quartz tube was evacuated with a Hg diffusion pump (10^{-6} torr) versus a mechanical pump (10^{-3} torr) before the tube was sealed to remove H_2O vapor.

(2) The quartz tube was heated to 1000°C under vacuum for 3 hours to fuse all open silanol sites and remove water present in the tube.

(3) Yb and $ZnBr_2$ were mixed in an argon filled glove-box fitted with a purification train which contained molecular sieves to remove H_2O and BASF catalyst to remove oxygen from the argon. Solid P_2O_5 was placed inside of the glove-box to further reduce the residual H_2O partial pressure.

(4) The quartz tube was cooled under vacuum after being heated to 1000°C for 3 hours. The tube was removed from the vacuum line with argon and Parafilm was immediately placed on the end. Then, the tube was placed in the glove-box with the Yb and $ZnBr_2$ reactants.

Possible reasons for YbOBr presence:

(1) Reaction of $YbBr_2$ with the quartz tube. Schafer[39] reported reaction of Al_2Cl_6 with a quartz tube at 300°C to produce AlOCl. At more elevated temperatures, Al_2O_3 is formed. A low temperature (400°C) preparation of $YbBr_2$ by use of a Pyrex tube instead of a quartz tube was attempted at MSU.

Yb and $ZnBr_2$ were added to the tube in the glove-box and the tube was sealed under vacuum. YbOBr was found by X.R.D.

(2) Any attempt at M.S.U. to produce SmI_2 showed that oxygen was present in the glove-box. A new BASF catalyst apparatus was prepared to remove oxygen from both the glove-box and the attached trap. A Na-K alloy was placed in the glove-box to remove the residual oxygen and water vapor. $YbBr_2$ could be more subject to hydrolysis or oxidation than the YbI_2 or $YbCl_2$ samples. Huheey[59] points out a number of unusual characteristics of those main group elements, in this case, bromine, which follow the first complete 3d block. In the $YbCl_2/YbI_2$ system, an alundum boat was used successfully to contain the samples during heating without oxidation. However, in the $YbBr_2/YbCl_2$ system, an alundum boat was used and a YbOBr impurity resulted.

(3) It was reported that water desorbed from the walls of a heated quartz tube.[51] This desorption occurred when the tube was sealed by a torch at temperatures in excess of 1000°C. Desorbed water could have hydrolyzed the $YbBr_2$ and produced YbOBr.

All samples prepared by method one ($Yb + ZnBr_2 \rightarrow YbBr_2$) contained YbOBr. Samples synthesized by method two, ($Yb + 2YbBr_3 \rightarrow 3YbBr_2$) did not show the presence of YbOBr (Table 10-083b/85). This observation is interpreted to mean that the source of oxygen is not the glove-box, but is either the quartz tube or moisture (oxygen) generated when the quartz tube was sealed off with a torch. Confirmation that $YbBr_2$ had indeed been prepared was difficult until a dissertation of one of Dr. Baernighausen's students[30], Dr. Bossert, was received. In this dissertation, four temperature dependent structure-types for $YbBr_2$ are reported.

Bossert used the high temperature Guinier X.R.D. technique to identify the four structure types. The equation suggested for their $YbBr_2$ synthesis was:

$$YbBr_3 \text{ (Ta container)} \xrightarrow{727°C-827°C} YbBr_2(s) + TaBr_5(g) + TaBr_{2.8}(s)$$

An important fact observed during Bossert's synthetic procedure was the presence of $TaBr_5$ and $TaBr_{2.5}$. An open tantalum crucible was filled with $YbBr_3$ and placed in an evacuated quartz tube. In the upper part of the quartz tube, an orange-red solid was found which was identified as $TaBr_5$. A darker solid was found closer to the $YbBr_3$ sample. This solid was amorphous by X.R.D. and by chemical means was found to be $TaBr_{2.5}$.

The $YbBr_2$ synthesized by Bossert was placed in the X.R.D. instrument and heated to 500°C. X-ray diffraction photographic films were taken at the following temperatures with the suggested structure types indicated:

SrI_2–207°C; α-PbO_2–267°C; $CaCl_2$–447°C and rutile–477°C.

Samples of $YbBr_2$ were prepared at MSU by the following methods:

1. $Yb(s) + ZnBr_2(l) \xrightarrow{550\ ^\circ C} YbBr_2(s) + Zn(g)$
2. $Yb(s) + 2YbBr_3(l) \xrightarrow{960\ ^\circ C} 3YbBr_2(s)$

All X.R.D. patterns of samples prepared by synthetic method 1 (Table 6) were the same as that of $YbBr_2$ listed in appendix 6. These $YbBr_2$ samples were a mixture of $CaCl_2$ and SrI_2 structure types. Neither α-PbO_2 nor rutile type $YbBr_2$ phases were found in samples prepared by method 1. By synthetic method 2, all X.R.D. patterns from samples (Table 6) showed X.R.D. patterns as seen in Appendices 3 and 5.

Method two was a high temperature (960°C) preparation so the high temperature forms of $YbBr_2$, $CaCl_2$ and rutile were expected. Samples 146-10-85 and 12-85 prepared by method 2 showed the SrI_2 structure. Whereas, 091a-85 and 079b-84 also prepared by method 2, showed a $CaCl_2$ and SrI_2 structure. A rationalization for presence of

only two structure types of $YbBr_2$ from the four known is found in x-ray diffraction discussion section.

In the first $YbBr_2$ preparation by method two (079b/84), the reaction took place at 1040°C for a 15 minute time period in a tantalum container. A red solid was produced and in addition, the tantanlum container expanded. This expansion may be due to formation of $TaBr_x$ compounds. Bossert[30] found that $TaBr_5$ and $TaBr_{2.5}$ were formed by the reaction of $YbBr_3$ with tantalum in an open evacuated container at 727°C. $TaBr_x$ compounds have similar physical properties to $TaCl_x$. Since the boiling point[54] of $TaCl_5$ is 233.9°C, the compound is gaseous at 1040°C. Therefore, it is likely that $TaBr_5$ is gaseous at 1040°C. Expansion of the sealed tantalum container is thus very predictable. Synthesis of $YbBr_2$ by method two at a temperature of 960°C (091a/84, 12/85) yielded only a green solid so no $TaBr_5$ was present and the tantalum tube did not expand. Some of the above facts are summarized below:

1. No tantalum-$YbBr_2$ reaction at 960°C.

2. A temperature difference between the tantalum-$YbBr_2$ reaction at MSU (1040°C) versus tantalum-$YbBr_3$ reaction of Bossert (727°C).

These results are probably due to the rate of heating. The $YbBr_2$ preparation at 960°C was heated at a very slow rate. The $YbBr_3$ reacted with Yb at a temperature far below 960°C and $YbBr_2$, once formed, does not react with tantalum. A faster rate of heating pursued for the 1040°C preparation caused $YbBr_3$ to react with the hot tantalum before it could react with Yb. The faster heating rate led to the formation of $TaBr_5$.

The low recoveries in some of the mixed halide systems were due to the adhesion of melt or powder to the graphite boat. Reaction with the graphite boats, all of which had a very smooth surface, was not observed.

DISCUSSION

X-Ray Diffraction

$YbBr_2$–$YbCl_2$ System. The standard deviations of the lattice parameters derived from the least-squares fit of the SrI_2-type Miller indices to the observed reflections were consistently less than ±0.009A for the $YbBr_2/YbCl_2$ system (see Table 11). Such a good fit is considered evidence that the SrI_2-type structure or some closely related modification thereof prevailed throughout the system. The presence of only the SrI_2 structure-type was unexpected since $YbBr_2$ synthetic preparations had yielded the $CaCl_2$ and SrI_2 structure-types. Thus, a rationalization for the presence of only the SrI_2 structure-type in this system is necessary.

The SrI_2 structure-type is the only reported structural form for $YbCl_2$.[40] In contrast, four know temperature dependent structure-types[30] are reported for $YbBr_2$. The highest temperature structural form is reported to be that of rutile (477°C), then at progressively lower temperatures the $CaCl_2$, α-PbO_2 and the lowest temperature form, SrI_2. Therefore, one reason that the SrI_2 structure-type might be favored is because it is the only structure-type common to both $YbCl_2$ and $YbBr_2$. Mixed chloride-bromide phases then, would be expected to exhibit the common SrI_2 structure-type. In addition, a rationalization for the presence of only two of the four known structure-types will be necessary to explain the $YbBr_2$ synthetic preparations. Such an explanation will be attempted here. Both the $YbBr_2/YbCl_2$ mixtures heated at 750°C, as expected, and the $YbBr_2$ preparations in tantalum

heated to 960°C for 15 minutes (146-10-85, 12-85) were found to exhibit only the SrI_2 structure-type. Other $YbBr_2$ preparations heated in tantalum to 1040°C for 15 min (079b/84; 091a/85) and to 550°C in quartz for 3 days exhibited both SrI_2 and $CaCl_2$ structure-types.

According to the data of Bossert, $YbBr_2$, on cooling, transforms from the $CaCl_2$ structure to the α-PbO_2 structure-type at 477°C, and from the α-PbO_2 structure-type to the SrI_2 structure-type at 100°C.[39] Thus if a preparation were cooled too quickly for equilibrium to be established, the resultant mixture would be expected to be that of the α-PbO_2 and the SrI_2-types, not the $CaCl_2$ and SrI_2-types. Some phenomenon other than thermodynamic equilibrium must be stabilizing the $CaCl_2$-type structure.

As stated previously, the $CaCl_2$ structure-type was observed in samples that had been heated for either extended time periods or at the highest temperature. A possible explanation might be the presence of an impurity phase. A tantalum impurity might have been introduced in the highest temperature preparation. Whereas, a silicon impurity may have been introduced in the low temperature preparation. However, such impurities would most likely have been less than 1 or 2 percent which is below the x-ray diffraction detection limit. These trace impurities in the $YbBr_2$ end product could have stabilized the $CaCl_2$ structure-type.

An alternative explanation for the presence of only two structure-types can be developed in terms of the Yb-Br crystal radii, coordination number of cation and anion, and geometry of anion coordination. Data relative to the four structure-types of $YbBr_2$ are summarized in Table 17.

Table 17. Average Yb-Br interatomic distances, coordination number of anion and cation, and geometry of bromide anions of the four structure-types for $YbBr_2$.

Structure-Type	d(Yb-Br)[30] (A)	Coordination Number		Anion Coordination Geometry
		Cation	Anion	
SrI_2	3.008	7	3	trigonal
		7	4	tetrahedral
$CaCl_2$	2.913	6	3	trigonal
α-PbO_2	2.920	6	3	trigonal
rutile	2.924	6	3	trigonal

Unfortunately, an ionic radius for three-coordinated bromide ions is not available, but it is safe to assume the radius is constant in all three-coordinated structure-types. From the Yb-Br interatomic distances listed in Table 17, the three high temperatures forms (rutile, $CaCl_2$, α-PbO_2) are seen to have essentially identical interatomic distances with the low temperature form (SrI_2) to have a slightly larger interatomic distance consistent with the higher coordination number. Thus of the four possible structure-types, three are almost identical; one is different. A slight kinetic stability edge must be present for the $CaCl_2$-type structure. This kinetic barrier could be shallow enough that under equilibrium conditions, the $CaCl_2$-type structure reverses to the α-PbO_2-type structure, and then to the SrI_2-type structure. But in a typical heating experiment where samples were quenched, the $CaCl_2$-type structure could not transform quickly enough.

A third explanation may be deduced from the laboratory observations and literature sources. In the laboratory when a slight excess of Yb metal was added to the tantalum tube (equation - $Yb + 2YbBr_3 \rightarrow 3YbBr_2$), the SrI_2-type $YbBr_2$ products were found to be a solidified green melt with some black product on top. This apparently less-dense black material could be a Yb^{2+} cation rich product. The black color could result from electrons being trapped in anion sites.

For $YbCl_2$, *only* the SrI_2-type structure is stable over the entire solid temperature range; whereas for $YbBr_2$ the same structure-type is stable over a very limited low temperature range. It can be inferred that the SrI_2-type structure is *more stable* as the ratio: radius cation/radius anion increases, i.e. $rYb^{2+}/rCl^- = rYb^{2+}/1.8\text{A}$ vs. $rYb^{2+}/rBr^- = rYb^{2+}/2.2\text{A}$ (The truthfulness of this hypothesis can be

verified by examining the $TmBr_2$ phase diagram, in which rTm^{2+}/rBr^- is larger than rYb^{+2}/rBr^-.)[30]

If an electron is substituted for the bromide ion in some of the anion sites, a feat which could happen if excess Yb dissolved in the molten $YbBr_2$ and the melt was cooled quickly, the average anion size would be decreased, so therefore the r_{cation}/r_{anion} ratio would *increase*. Then SrI_2-type structure would become more chloride-like and more stable. On the other hand, if Yb^{3+} is present as an impurity in the structure, the structure could accommodate the charge imbalance by leaving one Yb^{2+} cation site vacant for every two Yb^{3+} ion present in the structure (charge balance). The effect of both having the smaller Yb^{3+} ion on a Yb^{2+} cation site, and some cations absent from the structure, would be to decrease the effective size of the cation. Such a decrease in effective cation size would cause the ratio: r_{cation}/r_{anion} to *decrease*, and would further destabilize the SrI_2-type structure (i.e. lower the transition temperature possibly to below room temperature), making the $CaCl_2$-type structure, which apparently has a slight stability edge over the other two structural-types, the more stable form.

Results of the Yb-Br-I phase study, discussed later in this thesis, substantiate this size hypothesis. When the iodide ion is substituted for the bromide ion, the cation-anion ratio is effectively *decreased*, the SrI_2 structure is destabilized, and the $CaCl_2$-type structure is predicted to be stable. The $CaCl_2$-type structure was indeed observed. A Yb-Br-I phase with minimal iodide concentration, if cooled to liquid nitrogen temperatures, might be expected to exhibit the SrI_2-type structure.

Divalent thulium, which is slightly larger than divalent ytterbium transforms at 427°C from the SrI_2-type structure to the α-PbO_2

structure. Tm^{2+}, being larger than Yb^{2+}, would *increase* the r_{cation}/r_{anion} ratio, and the SrI_2-type structure should exist over a larger temperature range. As compared to Yb(II), the smaller calcium ion in $CaBr_2$ does not form either the SrI_2 or α-PbO_2-type structures. At room temperature, $CaBr_2$ exists as a $CaCl_2$ structure-type and under heating can be transformed only to the rutile structure.

A comparison of the $YbBr_2/YbCl_2$ system to other mixed halide systems will be undertaken. Of particular interest are strontium and calcium mixed halide systems because these two systems most closely resemble the present one. Beck[60] noted that under high pressure, stronium chloride (face centered CaF_2-type structure) transforms to the more dense, more highly coordinated $PbCl_2$-type.[63] Indeed the $PbCl_2$-type structure is commonly found not only in these, but in other mixed halide systems as well.[65] The reason for the formation of this structure probably resides in its greater density and higher coordination number. Mixed halide phases essentially create an internal pressure and thus favor high coordination.[65] One reason that the $PbCl_2$-type structure was not found in the $YbBr_2/YbCl_2$ system could be due to the short time (maximum - 3 minutes) at the final temperature of 750°C. The combination of the time, temperature and quench did not create an internal pressure sufficient for transformation to the $PbCl_2$ structure-type.

Next a comparison of Yb(II) halide system versus the Sr(II) and Ca(II) halide systems is necessary. The Yb(II) and Sr(II) halide systems are not similar because of their differing crystal radius size, that of Yb(II) - 1.22Å and that of Sr(II) - 1.35Å. However, if cation radius is the sole criterion the Yb-Cl-Br system should be comparable to that of

Ca-Cl-Br[66] because the crystal radius of Yb(II) (1.22Å) is approximately equal to that of Ca(II) (1.26Å). The Ca-Cl-Br system was reported to exhibit a single phase solid solution of pseudo-rutile-type structure. It would thus seem that in this instance the cation radius is an excellent predictor of system behavior. Another good predictor of mixed halide behavior has been high pressure structural modifications. Unfortunately such structural studies are not available for ytterbium halides, hence, prediction of mixed ion behavior based upon them cannot be made.

The observed volume change with composition presented in Figure 11, was expected since the smaller Cl anion was being replaced by a larger Br anion. However, Vegards' law is not obeyed in this system as can be seen by the nonlinearity in the region of high molar percent of $YbBr_2$. If this law were obeyed, each lattice parameter increase should be directly proportional to the increasing mole percent of $YbBr_2$. Variations from this law as indicated by the nonlinearity on the $YbBr_2$ side could be interpreted as evidence for ordering of the anions into the two anion sites as compared to random site occupancy.

To check for anion ordering, x-ray powder diffraction intensity calculations were effected with the program POWDER12[69] for the 75 and 55 mole percent bromide specimens. The results of these calculations are presented in Table 18. Three structural arrangements were considered:

1. random occupancy of the anion sites by both ions,
2. the bromide ion only in the tetrahedral site, and
3. the bromide ion only in the trigonal site.

For these calculations the structural and thermal parameters reported for $YbCl_2$ [40] were used in conjuction with lattice parameters derived in

Table 18. Comparison of observed and calculated intensities for low angle reflections in the $YbCl_2$-$YbBr_2$ system at the compositions: 0.25$YbCl_2$-0.75$YbBr_2$(A) and 0.45$YbCl_2$-0.55$YbBr_2$(B).

Composition	hkl	Intensity			
		obs	random	Br in X(1) (trigonal)	Br in X(2) (tetrahedral)
A	200	vw	4	0	10
	210	w	8	11	5
	111	vw	2	3	1
	211	vvs	100	100	100
B	200	w	4	0	17
	210	m	8	15	3
	111	vw	2	4	1
	211	vvs	100	100	100

this work. Polynomial scattering factors included in the program were used.[60] Neither an absorption correction nor anomalous dispersion terms were included in the calculations, but a correction was made for the incident beam monochromator.

On the basis of these observations it is clear that the anions do not uniquely occupy the tetrahedral hole, and it is probable that they do not uniquely occupy the trigonal site. The occupancy appears to be random. The absence of the larger bromide ion in only the trigonal site is not surprising since in the $YbCl_2$ structure the average Yb-Cl distance for the trigonal site is 0.07A less than that in the tetrahedral site.

As was noted on Table 3, the $YbCl_2$-$YbBr_2$ melts were cooled slowly to room temperature. It was found that rapid cooling of these samples produced broadened X.R.D. reflections. During rapid cooling, the molten samples solidified so quickly through the liquid-solid region to the solid region that a homogeneous composition did not result. Therefore, some parts of the solidified sample could be more chloride or bromide rich, a situation which would cause a slight variation in lattice parameters, and broadened X.R.D. lines.

An alternative explanation for the presence of broad X.R.D. reflections is the solidification of rapidly cooled molten samples into a semi amphorous, disordered solid. Slow cooling through the liquid-solid region would minimize this problem and produce a crystalline, ordered solid.

Still another explanation for broad X.R.D. lines can be given by the fact that $YbBr_2$ exhibits four temperature dependent forms; each of which has a unique X.R.D. pattern which is very closely related to that

of the other phases. In the rapidly cooled sample, small regions of high temperature structural forms may have been quenched and be present in addition to the SrI_2-type structure. It is possible that SrI_2-type and high temperature type reflections might be superimposed. Where superimposition occurred, broadened X.R.D. reflections would result.

For the $YbBr_2/YbCl_2$ system, interplanar d-values and relative intensities of unexplained reflections are tabulated in Appendix 4. Attempts were made to fit the various structure-types listed in Table 15 to these unexplained reflections. The interplanar d-values for the rutile, $CaCl_2$ and α-PbO_2 structure-types were compared to the unexplained interplanar d-values in the $YbBr_2/YbCl_2$ system. All three temperature dependent structure-types (rutile, $CaCl_2$, α-PbO_2) exist for $YbBr_2$. The interplanar d-values of the last two structures found in Table 15, YbOBr and YbOCl were compared because of the potential oxidation of $YbBr_2$ or $YbCl_2$. Reflections of these five structures did not match the unexplained reflections in this system.

The possibility that these reflections might be the result of superstructure from anion ordering was also considered even though x-ray intensity calculations indicated this to be an unlikely possibility. But because the lattice parameters are so large a doubling of any one leads to such a plethora of reflections that meaningful assignments could not be made. A final preparation of a 45 mole percent $YbBr_2$ sample which was made long after the original work was complete yielded an X.R.D. pattern where every reflection could be indexed on the basis of the SrI_2-type structure. It is thus believed that the spurious reflections belong to an impurity phase which is probably a hydrate

that occurred either during the preparatory or x-ray diffraction process.

$YbCl_2$-YbI_2 System. Four regions were identified in this system. These regions can be described as follows: from zero to 20 mole percent $YbCl_2$, a single phase solid solution region of CdI_2-type structure; from 20 to 45 mole percent $YbCl_2$, a two phase region with a new, unidentified phase designated A and a single phase CdI_2-type structure; from 45 to 60 mole percent $YbCl_2$, one solid phase A, and from 60 to 100 mole percent $YbCl_2$, a two phase region with phase A and a solid solution region of SrI_2-type structure. The presence of phase A is confirmed by the zero slope for volume and lattice parameters as observed in Figure 12 and also the presence of numerous reflections which could not be assigned to a structure in the X.R.D. pattern. Phase A reflections reached maximum intensity near the 50/50 $YbCl_2$-YbI_2 composition region.

The two phase regions described above are consistent with the phase rule: $F = C - P + 2$. (F = number of independent variables or degrees of freedom, C = number of components, and P = number of phases). This system contains three elements (Yb, Cl, I), but these are constrained to the compositions $YbCl_2$ and YbI_2, hence this must be considered a pseudo two component system. There is only one independent composition variable, Cl, since when one component is fixed, the other also is fixed (1-Cl). Substituting C = 2 into the phase rule and rearranging, one obtains

$$F + P = 2 + 2 = 4$$

Since measurements were made at atmospheric pressure and room temperature, the vapor pressure of the components is negligible.

Therefore, vapor pressure as a variable can be neglected, and one degree of freedom is lost. This assumption reduces the phase rule equation by one to: $F + P = 3$.

The number of degrees of freedom plus the number of phases thus is constrained to equal 3, and when one phase is present there are two variables, temperature and Cl composition; when two phases are present, there is only one variable, temperature.

Application of these conclusions to the $YbCl_2$-YbI_2 system indicates that for a single phase region two variables, temperature and composition, prevail; whereas for a two phase region only one variable, temperature, prevails. Thus in a two phase region, composition is fixed and lattice parameters will be invariant to yield a lattice parameter-composition curve of zero slope; whereas, in a single phase region composition is variable, and lattice parameters will change.

In the one solid phase region from zero to 20 mole percent $YbCl_2$, the cell volume is shown as a line with decreasing linear slope due to the fact that chloride ions are substituted for iodide ions in a CdI_2-type structure. As the chloride ion concentration in the CdI_2 lattice increases, the lattice parameters decrease because the chloride anion is smaller than the iodide anion.

When phase A grows in at 20 mole percent $YbCl_2$, two solid phases are present. The probable composition of the phase A is $YbCl_{1.2}I_{0.8}$ or 60 mole percent $YbCl_2$. This composition is based on the assumption that the break in the "a" lattice parameter curve at about 70 mole percent $YbCl_2$ does not represent a change from a two (solid) phase region to a single phase region. If a change to a single phase region does occur, then the composition of phase A would be $YbCl_{0.9}I_{1.1}$ or 45

mole percent $YbCl_2$, the median composition between the initial and final appearance of phase A.

The 50 mole percent $YbCl_2$ lattice parameter data are not included in Figure 12 because the standard deviation of each lattice parameter is greater than ± 0.02Å. This large deviation is probably due to phase A reflections superimposed on very weak YbI_2 reflections with the consequence of inaccurate determination of line positions.

The "a" lattice parameter can be interpreted to change at 70 mole percent $YbCl_2$. Such a variation can be rationalized with the aid of Figure 1, a drawing of the SrI_2 structure. In this figure, anion 2 occupies a tetrahedral site; whereas anion 1 occupies a trigonal site. The smaller balls represent the Sr atoms.

If one starts with pure $YbCl_2$, one can imagine an iodide ion substituting for a chloride ion in the SrI_2-type structure as the $YbCl_2/YbI_2$ melt is cooled. The CN VI crystal radius of the iodide ion (2.06Å) is 0.39Å larger than that of the chloride ion.[67] The space group of this structure and the atom site numbering scheme are identical to those used by Baernighausen, et al. in reporting the $YbCl_2$ structure.[40] The structural data for $YbCl_2$ can thus be viewed directly in this figure. In the $YbCl_2$ structure the distances between the anions labeled 1,1', and 1" are 3.83-3.89Å; those between the anions labeled 2,2',2" and 2'" are 3.35-3.36Å. The Yb-Cl(2) distances are slightly longer than the Yb-Cl(1) distance, probably an indication that Cl(2)-Cl(2) anion contact is preventing the Yb atom from closer contact with the site (2) anions. If the site 2 anions are in contact, it seems probable that the larger iodide anion will prefer to occupy site (1) positions when substitution occurs. Because of their shorter Yb-Cl(1) distance, the anions labeled (1) are

presumed to have strong metal-anion contacts and weaker anion-anion contacts. An iodide substituting in one of these sites would therefore increase the metal anion distance (the a parameter) more than the anion-anion distance (the b and c parameters).

However, if iodide ions were substituted for 30 percent of the chloride ions in the unit cell, the volume expansion expected on the basis of the CN VI anion radii,[67] with no structural rearrangement, would be $\{4\pi(2.06^3-1.67^3)/3\}$, 17Å^3 per iodide ion or 82Å^3 {0.30x16x17Å^3} per unit cell. How well this theoretical volume difference between the anions approximates the actual volume change of the unit cell can be determined from an analysis of the opposite end of the system where the presence of solid solution was confirmed. It was pointed out (Figure 12) that 20 mole percent $YbCl_2$ could be substituted for YbI_2 in the CdI_2-type structure. The formula of the unit cell of the 20 mole percent substituted material would be $YbI_{1.6}Cl_{0.4}$, and the volume change expected from the substitution is {0.2x2x17Å^3}, or 6.8Å^3. The observed volume charge of ~3Å^3 is about half this value, indicative not only of the extensive structural rearrangements that occur, but also that about a 40Å^3 (half of 82Å^3) volume change should occur if 30 mole percent substitution occurred at the chloride rich end.

The observed expansion of about 2Å^3 is totally inconsistent with this calculation, and leads to rejection of the hypothesis that iodide substitution has occurred to the 30 percent level. The composition of phase A is therefore inferred to be $YbCl_{1.2}I_{0.8}$ (60 mole percent $YbCl_2$), and only minimal iodide substitution must occur in the $YbCl_2$ structure.

Due to the presence of 25 unindexed reflections in the 20 to 65 mole percent $YbCl_2/YbI_2$ samples, the X.R.D. patterns of the various

structure-types listed in Table 16 were calculated and compared to these unassigned reflections. The $CaCl_2$, α-PbO_2, rutile, SrI_2, SrI_2(II) and YbOBr structure-types were considered because the radius of the Br anion is intermediate to that of the chloride and iodide anions.

The $PbCl_2$ structure-type was considered because it has been identified in some stronium halide systems as has been discussed in the $YbCl_2/YbBr_2$ X.R.D. discussion section. Two other structure-types, CdI_2 and $CdCl_2$ were considered because one member of the system, YbI_2 exhibits the CdI_2 structure-type. Since both $YbCl_2$ and YbI_2 are susceptible to oxidation, YbOCl and YbOI were considered. The very common PbFCl structure-type is found in compounds LaOI, LaClSe, ThOSe and ThOS which have ionic radii similar to those of YbClI.

The last structure listed, BiSI was considered because of results obtained from application of both the Hess-Lipson and Ito's procedures[56] to phase A reflections. These procedures yielded lattice parameters of a = 11.14, b = 9.47, c = 6.62A and β = 102.7°. Since these lattice parameters describe an RX_2 monoclinic cell, Wycoff[56] was searched for a similar structure and only BiSI was found. Ito's method[56] was also tried alone with the interplanar d-values that could be assigned to phase A reflections with the VAX program ITO-9.[58]

The necessary figure of merit of greater than 10 with 18 out of 20 lines indexed was not found. It is concluded that this phase A exhibits either a new or relatively uncommon type of structure.

<u>$YbBr_2$-YbI_2 System.</u> The results of six successful melt experiments run for this system are summarized in Table 14. These results may be described as follows: zero to 35 mole percent $YbBr_2$; a single phase CdI_2 structure-type and from 80-100 mole percent $YbBr_2$; a

single phase $CaCl_2$ structure-type. An increase in the percent bromine from zero to 35 mole percent $YbBr_2$ causes the size of the CdI_2-type lattice to decrease because the Br anion is smaller than the I anion. A similar result is seen when the 100 mole percent $YbBr_2$ sample is compared to the 80 and 85 mole percent $YbBr_2$ samples; the $CaCl_2$-type lattice is found to increase in size.

The results of the 35, 80 and 85 mole percent $YbBr_2$ samples, and the three remaining melt samples (45, 60 and 75 mole percent $YbBr_2$) are presented in Figure 13. These remaining melt samples were identified from the X.R.D. films as follows: 45 mole percent $YbBr_2$--new phase A; 60 mole percent $YbBr_2$--a two phase region with new phase A and new phase B; and 75 mole percent $YbBr_2$--a two phase region with one phase of the $CaCl_2$ structure-type and the other consistently of new phase B. The X.R.D. patterns of neither phase A nor phase B could be explained by either the CdI_2 or $CaCl_2$ structure-type.

An additional five melt samples were found to contain $YbBr_2/YbI_2(H_2O)_x$ as shown in Table 19. The 15, 25 and 30 mole percent $YbBr_2$ melt samples in which a single phase CdI_2 structure-type was found confirmed the earlier results of the zero to 35 mole percent $YbBr_2$ samples.

One result that needs comment is the presence of the $CaCl_2$ structure-type in the 80 and 85 mole percent $YbBr_2$ samples. As discussed in $YbCl_2$-$YbBr_2$ section, substitution of a larger iodide ion for a bromide ion is equivalent to decreasing the r_{cation}/r_{anion} ratio. It was postulated in the $YbCl_2/YbBr_2$ discussion section that as the r_{cation}/r_{anion} ratio decreases (i.e. compare radius ratio rYb^{2+}/rCl^- versus rYb^{2+}/rBr^-), the SrI_2-type structures destabilizes and a mixture

of $CaCl_2$ and SrI_2-type structures are exhibited. In the Yb-Br-I system, the radius ratio decrease may have destabilized the SrI_2-type structure because the $CaCl_2$-type structure alone was exhibited.

A literature reference to the existence of a YbI_2 hydrate was investigated. No reference for $YbI_2(H_2O)_x$ could be found, but hydrates of other divalent metal halide systems have been studied extensively. The monohydrate is found to be the most common among metal(II)-halide systems. The following monohydrates crystallize in an orthorhombic form with space group Pnma: $SrBr_2 \cdot H_2O$ [70], $EuBr_2 \cdot H_2O$ [70], $EuI_2 \cdot H_2O$ [71], $SmBr_2 \cdot H_2O$ [72], $BaCl_2 \cdot H_2O$ [73] and $SrCl_2 \cdot H_2O$.[74] The large differences in the cation/anion ratios of the above monohydrates would lead one to expect $YbI_2 \cdot H_2O$ to crystallize in the same easily indentified structure. On the other hand, the hemihydrates, $2BaCl_2 \cdot H_2O$ [73] and $2SrCl_2 \cdot H_2O$ [74] crystallize in a structure that has not been characterized. The interplanar d-values of the YbI_2 hydrate are reasonably similar to those of the two uncharacterized hemihydrates, but are very different from the well characterized monohydrates. The formula of the hydrate is therefore suspected to be $2YbI_2 \cdot H_2O$.

Table 19. Phases exhibited in $YbBr_2/YbI_2(H_2O)_x$ system.

Mole % $YbBr_2$	Phase
15	CdI_2-Type
25	CdI_2-Type
30	CdI_2-Type
40	New Phase A
42	New Phase A

Note: Phases determined by visual comparison of X.R.D. films in which the CdI_2-type structure and phase A were found. No d-values were calculated for the above samples. Therefore, no mole percent limit can be set for phase A.

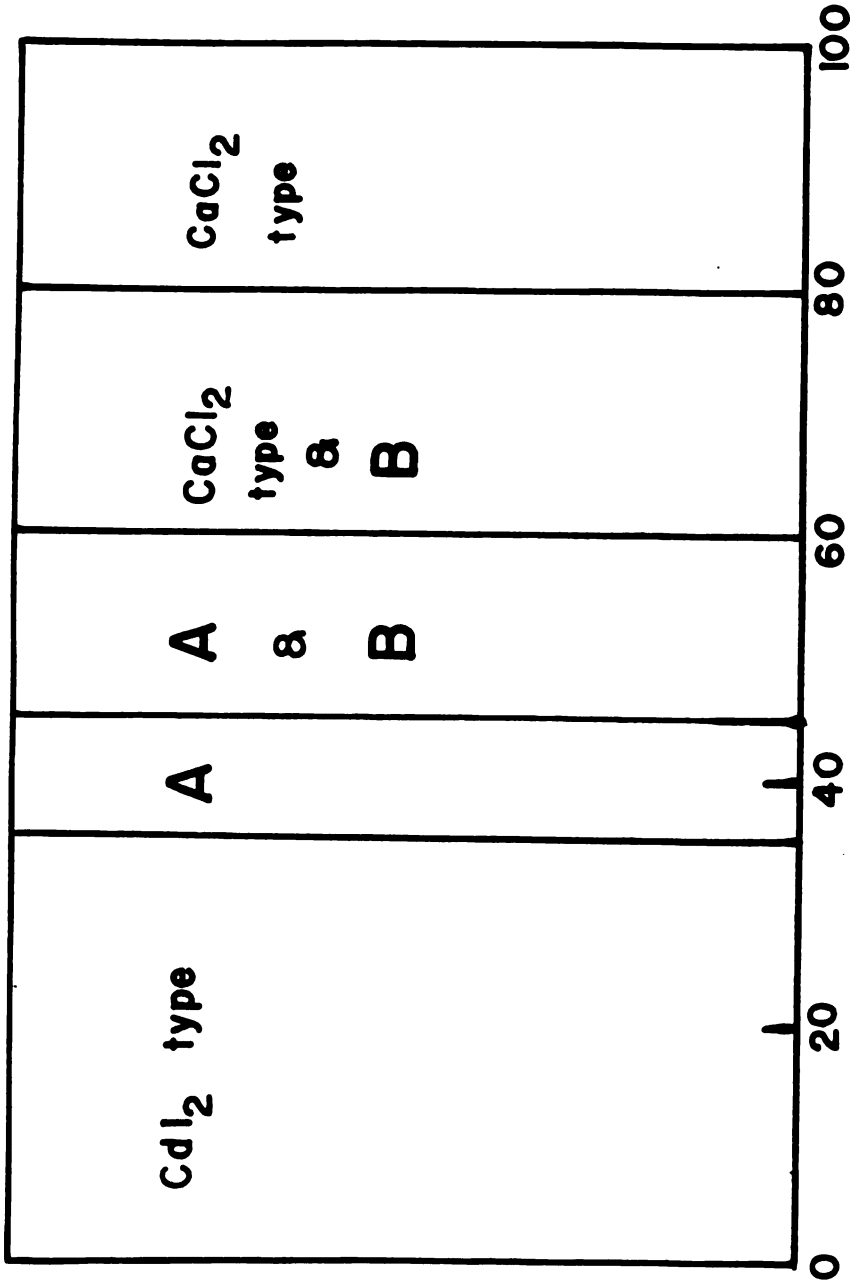

Figure 13. Structure Types for the $YbBr_2/YbI_2$ System.

Conclusion

Ytterbium mixed dihalide systems are compared to the europium(II) and calcium mixed halide systems. These comparisons are made because europium, like ytterbium, is a member of the lanthanide series of elements. Europium(II) has a half-filled f shell; whereas ytterbium(II) has a filled f shell. On the other hand, calcium and ytterbium(II) have the same size ionic radii.

The europium and ytterbium mixed dihalide systems are compared first. In the $YbCl_2$-$YbBr_2$ system, one solid solution of an SrI_2-type structure was found. The $EuCl_2$-$EuBr_2$ system[65] exhibited three regions: zero to 5 mole percent $EuCl_2$, a single phase $SrBr_2$-type structure; 5 to 15 mole percent $EuCl_2$; two phases indexed with lattice parameters of the terminal phases--5 mole percent $EuCl_2$ and 15 mole percent $EuCl_2$ and from 15 to 100 mole percent $EuCl_2$, a single phase $PbCl_2$ structure-type. One explanation for the differences between the above two systems may be attributed to the structure types of each individual lanthanide dihalide; i.e., for the Yb-Cl-Br system, both $YbCl_2$ and $YbBr_2$ exhibit an SrI_2 structure-type. For the Eu-Cl-Br system, $EuCl_2$ exhibits a $PbCl_2$ structure-type and $EuBr_2$ exhibits a $SrBr_2$ structure-type. In view of this evidence, a multiphase system would seem more likely to be found in the Eu-Cl-Br system in contrast to the Yb-Cl-Br system. The smaller ytterbium(II) ion apparently is able under the internal pressures created by the mixed anion system to accommodate both anions. Under higher pressures, the $PbCl_2$ structure-type would probably form. On the other hand, the calcium bromide-chloride system,[66] like that of ytterbium is characterized by one solid solution of pseudo TiO_2 structure-type. Each of parent phases, $CaBr_2$

and $CaCl_2$ exhibit the orthorhombic $CaCl_2$-type structure. From these data, it would seem that size constraints are the predominant predictor of structure-type.

The $YbCl_2$-YbI_2 system formed a total of four regions as follows: from zero to 20 mole percent $YbCl_2$, a single phase CdI_2-type structure; from 20 to 45 mole percent $YbCl_2$, two phases with phase A and a single phase of CdI_2-type structure; from 45 to 60 mole percent $YbCl_2$, a single phase labeled A and from 60 to 100 mole percent $YbCl_2$, two phases--one labeled A and the other an SrI_2-type structure. The Eu-Cl-I system[61] formed three principal regions as follows: from 0 to 50 mole percent $EuCl_2$, two phases both with lattice parameters typical of $PbCl_2$-type structures; 50 mole percent $EuCl_2$, a $PbCl_2$-type structure and from 50 to 100 mole percent $EuCl_2$, two phases with $PbCl_2$-type structures. The parent phases are as follows: $EuCl_2$, $PbCl_2$-type structure and EuI_2, both the SrI_2-type structure and an m-EuI_2 structure. A $PbCl_2$-type structure did not form in the Yb-Cl-Br system, and it was not found to correspond to phase A of the Yb-Cl-I system. Even in the absence of the structural type exhibited by phase A, it is apparent that these systems are very different. In contrast, the Ca-Cl-I system[66] contains three regions, from 0 to 5 mole percent $CaCl_2$, CdI_2 structure-type; from 5 to 97.5 mole percent $CaCl_2$, two phases - CdI_2 and $CaCl_2$, and from 97.5-100 mole percent $CaCl_2$, $CaCl_2$ structure-type. While the Yb-Cl-I and Ca-Cl-I systems are similar at the iodide end, there is a significant difference between these two systems at the chloride end. Also, the presence of a discrete, unique phase of intermediate composition was found in the Yb-Cl-I system and no new phase was found in the Ca-Cl-I system. This difference in behavior points out, (in contrast to the

apparent conclusion derived from the Yb-Cl-Br system) that radius ratio or size is not the sole criterion in determining the structures of mixed halides.

The complexity of the Eu-Br-I system[61] with seven distinct regions is similar to that of the Yb-Br-I system with five distinct regions. A comparison between the two solid solution regions found in the Yb-Br-I versus the Ca-Br-I systems are as follows: one solid solution region of $CaBr_xI_{2-x}$, from $0 < x < 0.4$ versus $YbBr_xI_{2-x}$, from $0 < x < 0.7$ and a second region of $CaBr_{2-y}I_y$, from $0 < y < 0.2$ versus $YbBr_{2-y}I_y$, from $0 < y < 0.4$. Outside of these solid solution regions a two phase region is exhibited in the Ca-Br-I system and is composed of the terminal phases. It is interesting to note that the solid solution region in the ytterbium system is much greater at both ends than in the calcium system. In this case, size is not a factor because the coordination number six radii indicate only a 0.02A difference between Yb(II)-1.16A versus Ca(II)-1.14A[67] In addition, two new uncharacterized phases occur in the ytterbium system, while there is no new phase formation in the calcium system.

In conclusion, the results presented in this thesis indicate both radius ratio alone (i.e., Yb-Cl-I versus Ca-Cl-I) and high pressure structure types alone (i.e., Yb-Cl-Br versus Eu-Cl-Br) to be poor criteria to use to analyze the behavior of mixed halide systems. However, Pearson's hard/soft acid-base theory may help explain the behavior of the Yb-Cl-Br system versus those of the comparable Eu(II) and Ca(II) systems.

In the Ca-Cl-Br system, a pseudo TiO_2 structure was exhibited with a coordination number for the calcium ion of six and a 1.14A size.[67]

The Yb-Cl-Br system also exhibited only one SrI_2-type phase in which the coordination number of the ytterbium is 7 with a 1.22A size.[67] A $PbCl_2$-type structure was found in the Eu-Cl-Br system (from 15 to 100 mole percent $EuCl_2$) where the cation coordination number is nine with a 1.44A size. Therefore, the actual sizes of the atoms are significantly different.

In an extrapolation of Pearson's theory, a small size cation like Ca(II) in the Ca-Cl-Br system can be equated to "hardness", whereas a larger ion like Eu(II) can be equated to "softness" and be more able to form covalent-like bonds as compared to Ca(II). The "softer" the ion is, the more easily it will deform, and therefore, allow multiple phase formation to occur as was found in the Eu-Cl-Br system. On the other hand, the "hard" calcium(II) ion should not be susceptible to the internal pressure from mixed halide size difference and should not form multiple phases. This is confirmed by the fact that only one phase is exhibited in the Ca-Cl-Br system.

FUTURE EXPERIMENTS

In all three ytterbium dihalide systems further work should be done. The question of whether the anion site occupancy of the Yb-Cl-Br system is random or ordered should be clarified definitively. This determination can be made most convincingly by line profile analysis of digital x-ray powder intensity data.

The new phase, labeled A, which was observed in the Yb-Cl-I system should be characterized. X-ray positional and intensity data should be made from a melt of a 55 mole percent YbI_2 sample because the new phase is presumed "pure" at that composition. The composition of the YbI_2 hydrate should be determined. In order to eliminate formation of the $YbI_2 \cdot (H_2O)_x$ in the YbI_2 synthesis, the Pyrex tube must be completely freed of absorbed water. The mercuric iodide should be sublimed and mixed with small pieces of ytterbium in an absolutely dry glove box.

In the Yb-Br-I system the two new phases labeled A and B should be characterized by mixing a 40-42 mole percent $YbBr_2$ sample to identify phase A and by mixing a 65 mole percent $YbBr_2$ sample to identify phase B. Since the 55 mole percent $YbBr_2$ sample is a mixture of phases A and B, this mixture may help confirm the finding of the 40 and 65 mole percent $YbBr_2$ melt samples.

The hypothesis that the $CaCl_2$-type $YbBr_2$ structure is stabilized by ytterbium(III) impurities may be tested by spectrophotometric techniques. Properties of oxygen free aqueous and aqueous-ethanol solutions of ytterbium(II) have been studied spectrophotometrically, so

therefore, ytterbium(III) might be identified with this technique.[33] A second hypothesis stating that elemental ytterbium can be dissolved in $YbBr_2$, should be tested. If electrons are indeed trapped in anion sites or at F-centers, this material may exhibit semiconducting properties.

REFERENCES

1. M. D. Taylor, Chem. Rev., 62, 503(1962).

2. M. D. Taylor and C. P. Carter, J. Inorg. Nucl. Chem., 24, 387(1962).

3. O. G. Polyachenok and G. I. Novikov, J. Gen. Chem. U.S.S.R., 33(3), 2725(1963).

4. L. B. Asprey, T. K. Keenan and F. H. Kruse, Inorg. Chem. 3, 1137(1964).

5. O. G. Polyachenok and G. I. Novikov, Russ. J. Inorg. Chem., 9, 429(1964).

6. L. B. Asprey, T. K. Keenan and F. H. Kruse, "Proc. Conf. Rare Earths," Phoenix, Arizona, 1964, pp. 527-34.

7. D. T. Cromer, private communication.

8. J. K. Howell and L. L. Pytlewski, J. Less Comm. Metals, 18, 437(1969).

9. J. K. Howell and L. L. Pytlewski, J. Less Comm. Metals, 19, 399(1969).

10. C. W. DeKock and D. D. Radtke, J. Inorg. Nucl. Chem., 32, 3687(1970).

11. K. E. Johnson and J. R. MacKenzie, J. Inorg. Nucl. Chem., 32, 43(1970).

12. J. D. Corbett, Inorg. Nucl. Chem. Lett., 8, 337(1972).

13. F. L. Carter and J. F. Murray, Mater. Res. Bull., 7, 519(1972).

14. "International Tables for X-Ray Crystallography," Vol. IV, Kynoch Press, Birmingham, England (1974).

15. H. Baernighausen, H. P. Beck and H. W. Grueninger, "Proc. Rare Earth Res. Conf." Vol. I, 1971, p. 74.

16. H. Baernighausen and H. P. Beck, Z. Anorg. Allg. Chem., 386, 221(1971).

17. J. M. Haschke, "Handbook on the Physics and Chemistry of Rare Earths," North Holland Publishing Co., Vol. IV, New York, New York, 1979, p. 89.

18. N. B. Mikheev, A. N. Kamenskaya, N. A. Konovalova and T. A. Zhilina, Russ. J. Inorg. Chem., 22, 955(1977).

19. A. N. Kamenskaya, N. B. Mikheev and N. A. Konovalova, Russ. J. Inorg. Chem., 22, 1152(1977).

20. V. F. Goryushkin, A. I. Poshevneva and D. M. Lapter, Russ. J. Inorg. Chem., 27, 140(1982).

21. P. Girard, J. L. Namy and H. B. Kagan, J. Amer. Chem. Soc., 102, 2693(1980).

22. G. B. Deacon and A. J. Koplick, Inorg. Nucl. Chem. Lett., 15, 263(1979).

23. P. L. Watson, J. Chem. Soc., Chem. Comm., 652(1980).

24. H. Imamura, A. Ohmura and S. Tsuchiya, Chem. Lett. 203, (1984).

25. J. L. Namy, P. Girard and H. B. Kagan, Nouv. J. Chim., 5, 479(1981).

26. D. M. Laptev, A. I. Poshevneva and V. F. Goryushkin, Russ. J. Inorg. Chem. 27, 1229(1982).

27. G. B. Deacon, P. I. Mackinnon and T. D. Tuong, Aust. J. Chem., 36, 43(1983).

28. W. B. Jensen, J. Chem. Educ. 59, 634(1982).

29. A. K. Molodkin, A. M. Karagodina, A. G. Dudareva, A. G. Krokhina and V. S. Tupolev, Russ. J. Inorg. Chem., 29, 14(1984).

30. W. Bossert, Ph.D. Thesis, University of Karlsruhe, Germany, 1981.

31. L. B. Asprey and B. B. Cunningham, Prog. Inorg. Chem., 8, 267(1960).

32. J. D. Corbett, Rev. Chim. Miner., 10, 239(1973).

33. A. N. Kamenskaya, N. B. Mikheev and A. I. Strekalov, Russ. Inorg. Chem., 28, 965(1983).

34. O. G. Polyachenok and G. I. Novikov, Russ. Inorg. Chem., 8, 1378(1963).

35. A. N. Kamenskaya, K. Bukietynska, N. B. Mikheev, V. I. Spitsyn and B. Jezowska-Trzebiatowska, Russ. Inorg. Chem., 5, 633(1979).

36. D. A. Johnson, "Advances in Inorganic Chemistry and Radiochemistry," Vol. 20, Academic Press, New York, 1977, pp. 1-131.

37. W. Klemm and W. Schuth, Z. Anorg. Allg. Chem., 184, 352(1929).

38. J. L. Namy, P. Girard and H. B. Kagan, Nouv. J. Chim., 1, 5(1977).

39. H. Schafer, Z. Anorg. Allg. Chem., 445, 129(1978).

40. H. Baernighausen, Z. Anorg. Allg. Chem., 403, 45(1974).

41. L. B. Asprey and F. H. Kruse, J. Inorg. Nucl. Chem., 13, 32(1960).

42. N. A. Fishel and H. A. Eick, J. Inorg. Nucl. Chem., 33, 1198(1971).

43. J. K. Howell and L. L. Pytlewski, J. Appl. Crystallogr., 3, 193(1970).

44. Powder Diffraction File, Inorganic Phases, Alphabetical Index, JCPDS International Centre for Diffraction Data, Swarthmore, Penn., 1983.

45. D. E. Cox and F. K. Fong, J. Cryst. Growth, 20, 233(1973).

46. D. F. Evans, G. V. Fazakerley and R. F. Philips, J. Chem. Soc. A., 1931(1971).

47. R. S. Mitchell, Z. Kristallogr., 108, 296(1956).

48. E.Th. Rietschel and H. Baernighausen, Z. Anorg. Allg. Chem., 368, 62(1969).

49. P. Gordon, "Principles of Phase Diagrams in Materials Systems," McGraw-Hill Book Company, New York, 1968.

50. G. Brandt and R. Diehl, Mater. Res. Bull., 9, 411(1974).

51. G. Schmidt and R. Gruehn, J. Cryst. Growth, 57, 585(1982).

52. CRC Handbook of Chemistry and Physics, 58th Ed., CRC Press Inc., Cleveland Ohio(1978).

53. D. Brown, "Halides of Lanthanides and Actinides," J. Wiley-Interscience Publication, New York, 1968, p. 151.

54. J. of Phy. and Chem. Ref. Data, 7, 892(1978).

55. JANAF Tables, Second Edition, United States Department of Commerce, Washington D.C.

56. R. W. G. Wycoff, "Crystal Structures," Second Ed., Vol. 1, Interscience Publishers, New York, 1963.

57. A. V. Hariharan and H. A. Eick, High Temp. Sci., 4, 379(1972).

58. J. W. Visser, J. Appl. Cryst., 2, 89(1969).

59. J. E. Huheey, "Inorganic Chemistry," Third Ed., Harper and Row, New York, 1983.

60. H. P. Beck, Z. Anorg. Allg. Chem., 459, 72(1979).

61. E. K. Hodorowicz, S. A. Hodorowicz and H. A. Eick, J. Solid State Chem. **52**, 156(1984).

62. S. A. Hodorowicz and H. A. Eick, J. Solid State Chem. **46**, 313(1983).

63. S. A. Hodorowicz and H. A. Eick, J. Solid State Chem., **43**, 271(1982).

64. R. M. Bozorth, J. Amer. Chem. Soc., **44**, 2232(1922).

65. E. K. Hodorowicz, S. A. Hodorowicz and H. A. Eick, J. Solid State Chem., **49**, 362(1983).

66. S. A. Hodorowicz, E. Hodorowicz and H. A. Eick, Crystal Res. and Technol., **19**, 1377(1984).

67. R. D. Shannon, Acta. Cryst., **A32**, 751(1976).

68. B. G. Hyde, L. A. Bursill, M. O'Keeffe, S. Anderson, Nature (London) Phys. Sci., **237**, 35(1972).

69. D. K. Smith, M. C. Nichols and M. E. Zolensky, "A FORTRAN IV program for Calculating X-Ray Powder Diffraction Pattern-Version 10." The Pennsylvania State University, University Park, PA (1983).

70. J. M. Haschke and H. A. Eick, J. Inorg. Nucl. Chem. **32**, 2153(1970).

71. J. M. Haschke, Inorg. Chem., **15**, 508(1976).

72. J. M. Haschke, Inorg. Chem., **15**, 298(1976).

73. H. D. Lutz, W. Becker, Ch. Mertins and B. Engelin, Z. Anorg. Allg. Chem., **457**, 84(1979).

74. H. D. Lutz, B. Frischemeier, Ch. Mertins and W. Becker, Z. Anorg. Allg. Chem., **441**, 205(1978).

Appendix 1. Interplanar d-spacings and relative intensities observed for $YbCl_2$ (068b/84) versus those calculated from literature data.

d	i	hkl[a]	d[a]	i[a]
6.58488	W	200	6.5750	3.8
4.78099	W	210	4.7737	7.6
4.53132	W	111	4.5242	1.9
3.88408	S	211	3.8864	100.0
3.47686	M	020	3.4710	10.3
3.35061	M	002	3.3465	14.5
3.29273	W	400	3.2875	9.4
3.24893	W	102	3.2431	2.5
3.09338	W	021	3.0813	3.7
3.01135	W	121	3.0000	2.4
2.97535	W-	410	2.9712	1.7
2.79906	W	221	2.7901	3.3
2.74637	M	212	2.7402	7.2
2.71900	M	411	2.7156	9.5
2.66593	W	302	2.6599	3.1
2.41321	M	022	2.4091	21.1
2.38898	M	420	2.3868	17.0
2.34727	M	402	2.3452	19.3
2.31245	W-	511	2.3085	0.0
2.26832	W	222	2.2621	3.4

Appendix 1 continued.

d	i	hkl[a]	d[a]	i[a]
2.25133	M	421	2.2482	9.4
2.22621	W-	412	2.2218	1.1
2.18750	M	230	2.1828	10.7
2.10354	W	113	2.0968	2.5
2.07955	M	231	2.0752	12.1
2.02388	M	213	2.0212	17.6
1.99600	M	611	1.9950	19.3
1.94756	M	422	1.9432	7.1

a. Computer program ANIFAC, l.p.-ref. 40; p. 46 and atomic parameters-ref. 40; p. 48.

Appendix 2. Interplanar d-spacings and relative intensities observed for the $YbBr_2(55)/YbCl_2(45)$ melt sample.

d	i	hkl
6.77526	W	200
4.91763	M	210
4.68883	W-	111
3.99197	Sb	211
3.58427	W	020
3.43388	Wb	002
3.38868	W	400
3.32947	W-	102
3.11459	W	121
3.06322	W	410
2.87592	W	221
2.79216	Wb	411
2.73169	W	302
2.48119	M	022
2.45905	M	420
2.40826	Wb	402
2.31844	Wb	421
2.25405	M	230
2.13966	M	231
2.07581	W-	213
2.05162	M	611
2.00399	W-	422

Appendix 2 continued.

d	i	hkl
1.96626	W-	313
1.91050	W-	620
1.88499	W	602
1.84393	W-	621
1.73346	W	240
1.64806	W-	810
1.60871	W	304
1.54513	W	441

b = broad

Appendix 3. Interplanar d-spacings and their relative intensities of the $YbBr_2$ (146-10-85E) sample and theoretical values calculated for SrI_2-type $YbBr_2$ from literature data.

d	i	hkl[a]	d[a]	i
6.878	W	200	6.8993	8.2
5.0259	W	210	5.0331	11.2
4.7789	W-,b	111	4.7895	4.4
4.3260	?	---	---	---
4.0973	S++	211	4.1048	100.0
3.6729	W+	020	3.6794	6.3
3.5438	W+	002	3.5467	14.8
3.4482	?	400	3.4497	5.2
3.2454	W+	220	3.2465	8.8
3.1753	Wb	121	3.1783	11.5
3.1211	M-	---	---	---
3.0089	?	---	---	---
2.9486	M	221	2.9520	17.5
2.8959	Mb	212	2.8992	26.5
2.8553	M	411	2.8586	32.2
2.8043	Wb	302	2.8087	12.4
2.5525	S	022	2.5535	47.1
2.5158	S	420	2.5166	28.7
2.4703	Mb	402	2.4729	32.0
2.3930	Wb	222	2.3947	13.2
2.3692	Wb	421	2.3717	20.7

Appendix 3 continued.

d	i	hkl[a]	d[a]	i
2.3101	S	230	2.3112	31.3
2.2213	W	113	2.2217	9.7
2.1964	M	231	2.1975	16.5
2.1383	M[b]	213	2.1401	22.8
2.0957	M	611	2.0970	37.8
2.0206	W	313	2.0219	6.0
1.9881	W	023	1.9891	3.6
1.9685	W	123	1.9688	8.9
1.9501	W	620	1.9502	3.3
1.9351	W[b]	232	1.9363	10.5
1.7814	W-	041	1.7808	5.0
1.7777	W-	240(?)	1.7776	5.4

a. Computer program ANIFAC, l.p.-ref. 17; p. 119 and atomic parameters-ref. 48, p. 63.

b = broad

Appendix 4. Intensities and interplanar d-values of unexplained reflections observed in the $YbBr_2/YbCl_2$ system and compiled as a function of mole percent $YbBr_2$.

25	40	65	75	85	95
10.24211 W-	9.57574 M^b	4.28260 W	4.28142 M	4.58981 W-	5.17943 W
	5.91766 W				
4.00469 W-	4.6455 W	4.17544 W-	4.17452 W	4.31368 W-	4.34035 W-
3.90287 W-	3.93491 W	3.87189 W	3.86998 W	3.90971 W-	4.22099 W-
3.50459 W-	3.91366 W	3.03140 W-	2.97549 W	3.01004 W-	3.92089 W-
2.87539 W-	3.614321 W	2.98403 W-	2.72451 W-	2.20217 W	2.75929 W-
2.63658 W-	3.37264 W	2.77054 W-	2.40687 W-	1.40086 W-	2.56218 M
2.41356 M	2.77931 M	2.72393 W-	2.21834 W-		2.31947 W-
2.35896 W-	2.67684 W-	2.54060 W-	2.14102 W-		2.18277 W-
2.34748 W	2.43571 W	2.35862 W-	1.68977 W-		1.40306 W
	2.38701 W-				
2.27740 W	2.37673 W-		1.38694 W-		1.38256 W-
2.21008 W	1.93131 W		1.36390 W-		1.37679 W-
2.03144 M	1.55098 W-				1.36389 W-
1.94591 W	1.46975 W^b				
1.89330 W-	1.42966 W^b				
1.83507 W-					
1.53890 W-					
1.51277 W-					

Note: b represents a broad reflection line.

Appendix 5. $Sin^2\theta$, interplanar d-spacings and relative intensities for $YbBr_2$ (083b-85) with h,k,l's from literature data.

$Sin^2\theta$	d	i	hkl
0.00836	8.42381	W-	
0.02228	5.16020	W-	
0.02590	4.78640	S[b]	110-$CaCl_2$(a)
0.03512	4.10998	W	211-SrI_2(b)
0.04333	3.70025	M	011-$CaCl_2$(a)
0.04449	3.65188	S	101-$CaCl_2$(a)
0.04927	3.47002	W	020-$CaCl_2$(a)
0.05734	3.21677	S	111-$CaCl_2$(a)
0.06035	3.13521	Si	none
0.06301	3.06855	M	120-$CaCl_2$(a)
0.06492	3.02306	W	
0.07159	2.87875	W	411/212 SrI_2(b)
0.07997	2.72378	W	
0.08921	2.57881	W	
0.09085	2.55544	W	022-SrI_2(b)
0.09399	2.51238	S	420-SrI_2(b)/121-$CaCl_2$(a)
0.09785	2.46236	S	211-$CaCl_2$(a)
0.10026	2.43258	W	
0.10365	2.39250	S	222-SrI_2(b)/220-$CaCl_2$(a)
0.11043	2.31783	W	
0.12445	2.18341	S	002/130-$CaCl_2$(a)
0.12942	2.14109	W	213-SrI_2(b)
0.13420	2.10258	W	611-SrI_2(b)/310-$CaCl_2$(a)

Appendix 5 continued.

$Sin^2\theta$	d	i	hkl
0.14262	2.03958	S	031-$CaCl_2$(a)
0.14995	1.98912	M	112-$CaCl_2$(a)
0.15328	1.96740	M	123-SrI_2(b)
0.15857	1.93432	W	232-SrI_2(b)
0.16092	1.92032	Si	none
0.16570	1.89224	W	311-$CaCl_2$(a)
0.17158	1.85953	W	320-$CaCl_2$(a)
0.17318	1.85089	W-	022-$CaCl_2$(a)
0.18719	1.78031	W	122-$CaCl_2$(a)
0.20286	1.71015	W	321-$CaCl_2$(a)
0.21101	1.67678	W-	140-$CaCl_2$(a)
0.21821	1.64891	Wb	233-SrI_2(b)
0.22127	1.63709	Si	none
0.22814	1.6121	M	222-$CaCl_2$(a)
0.23344	1.59419	W	330-$CaCl_2$(a)
0.24272	1.56344	W	141-$CaCl_2$(a)
0.24922	1.54291	W	132-$CaCl_2$(a)
0.25294	1.53151	W	240-$CaCl_2$(a)
0.25953	1.51194	W	312-$CaCl_2$(a)
0.26045	1.50928	W-	411-$CaCl_2$(a)
0.26622	1.49284	W-	420-$CaCl_2$(a)
0.29199	1.42547	W-	103-$CaCl_2$(a)
0.29629	1.41506	W-	322-$CaCl_2$(a)
0.30568	1.39316	W-	113-$CaCl_2$(a)

Appendix 5 continued.

$Sin^2\theta$	d	i	hkl
0.31713	1.36777	W-	340-$CaCl_2$(a)
0.32185	1.35819	Si	none
0.38220	1.24566	Si	none

a. a.p. Reference 30, page 25; l.p., Reference 15, page 79.

b. a.p. Reference 48, page 63; l.p. Reference 17, page 119.

Note: no rutile as $YbBr_2$ (Reference 30); α-PbO_2 as $YbBr_2$ (Reference 30); Ta (Reference 44); $TaBr_{2.83}$ (Reference 44); $TaBr_5$ (Reference 44).

Appendix 6. $Sin^2\theta$, interplanar d-spacings and relative intensities for $YbBr_2$ (064b/84) with hkl's from literature data.

$sin^2\theta$	d	I	hkl
0.00867	8.27167	W	
0.01246	6.89907	W-	
0.01767	5.79495	W-	
0.02246	5.13988	W-	
0.02349	5.02530	W-	
0.02606	4.77156	S	110-SrI_2(b)/110-$CaCl_2$(a)
0.03151	4.33887	W-	
0.03318	4.22851	W-	
0.03535	4.09671	S	
0.04344	3.69546	M	011-SrI_2(b)/011 $Cacl_2$(a)
0.04472	3.64230	S	101-SrI_2(b)/101 $CaCl_2$(a)
0.04729	3.54192	W	
0.04946	3.46337	W-	020-$CaCl_2$(a)
0.04987	3.44900	W-	101-YbOBr(c)
0.05714	3.22214	S	111-SrI_2(b)/111-$CaCl_2$(a)
0.05896	3.17206	W	
0.06035	3.13580	Si	none
0.06081	3.12355	W-	
0.06314	3.06528	M	120-SrI_2(b)/120-$CaCl_2$(a)
0.06806	2.95240	W-	
0.06959	2.91974	W	
0.07041	2.90277	W-	
0.07266	2.85748	W	
0.07572	2.79919	M	102-YbOBr(c)

Appendix 6 continued.

$\sin^2\theta$	d	I	hkl
0.08277	2.67735	M	110-YbOBr(c)
0.09109	2.55208	M	
0.09432	2.50795	S	121-SrI_2(b)/121-$CaCl_2$(a)
0.09822	2.45766	S	211-SrI_2(b)/211-$CaCl_2$(a)
0.10053	2.42937	W⁻	
0.10401	2.38835	M	220-SrI_2(b)/220-$CaCl_2$(a)
0.10544	2.37211	W	
0.11118	2.30999	W	
0.11449	2.27637	W⁻	
0.11679	2.25390	W⁻	
0.11837	2.23874	W⁻	103-YbOBr(c)
0.11994	2.22406	W⁻	
0.12259	2.19987	W⁻	002-$CaCl_2$(a)

a. a.p. Reference 30, page 25; l.p. Reference 15, page 79.

b. a.p. Reference 48, page 63; l.p. Reference 17, page 119.

c. Reference 44, page 1039.

Note: No α-PbO_2 as $YbBr_2$ (Reference 30); rutile as $YbBr_2$(Reference 30); Zn (Reference 44); $ZnBr_2$ (Reference 56).